Quantifying the Value and Communicating the Protective Services of Nature-Based Flood Mitigation using Flood Risk Assessment

Technical Report, Draft 2.0

Authors

Orton, P.[1], MacManus, K.[2], Sanderson, E.[3], Mills, J.[2], Giampieri, M.[3], Fisher, K.[3], Yetman, G.[2], Doxsey-Whitfield, E.[2], Hugens, D.[2], Wu, Z.[1], Yin, L.[1], Georgas, N.[1] and Blumberg, A.[1], 2016.

Affiliations

[1] Stevens Institute of Technology, Davidson Laboratory

[2] Columbia University Center for International Earth Science Information Network (CIESIN)

[3] Wildlife Conservation Society

Research funded under the National Oceanic and Atmospheric Administration Coastal Ocean Climate Applications program, award NA13OAR4310144.

Project Summary

Municipalities across the nation are weighing the value of nature-based flood mitigation strategies and the ecosystem services they provide, yet there is limited quantitative information available to help inform these decisions. In this study, we use hydrodynamic model-based flood mapping and risk assessment to develop new nature-based flood adaptation concepts, quantify their value, and map their flood protection services. A case study of Jamaica Bay, New York City (NYC) is utilized where the recent impacts of Hurricane Sandy have created strong public support for flood mitigation measures.

The project's first year was a research and public input period. An analysis of historical change was used reconstruct historical landscapes, and models were created for present-day, 1609 and 1877 bay landscapes. A flood mitigation workshop was held with government agency representatives, urban planners, designers, scientists, and the general public, to take input on an initial set of concepts and allow for new ideas to be contributed. Over the subsequent months, nearly 40 flood mitigation concepts were evaluated using simulations of Hurricane Sandy and a Category-3 hurricane. A few important findings were (a) that marsh island restoration activities in the center of the bay do not reduce storm tides, and (b) storm tides were reduced by the 1877 inlet as they propagated into Jamaica Bay, whereas the much wider and deeper present-day inlet causes little if any reduction.

The second and final year of the project was dedicated to flood risk/mitigation analysis, benefit-cost analysis, and web mapper development. Three final mitigation scenarios that mimic the flood resistance of the 1877 inlet were chosen for deeper analysis. For these, a full flood risk assessment using a set of 144 storm simulations was used to estimate the annual probabilities for different flood heights and damages across the Bay's floodplain. These data were then used to evaluate the monetary benefits of each adaptation measure for a benefit-cost analysis.

The resulting data were used to populate an online flood mapping tool, AdaptMap, which shows flood area and depth for various storm return periods and lets the user select future sea level scenarios and future flood mitigation scenarios to view how flood zones will change. The mapper also includes flood mapping for the two historical landscapes, 1609 and 1877. GIS flood data and flood mitigation benefit-cost analysis data are available for user download, and animations may be viewed for each flood return period, sea level and mitigation scenario.

Key results of the project include (1) creation of Jamaica Bay estuary models for present-day and historical landscapes, (2) development of novel, cost-effective strategies for nature-based flood mitigation in an urban harbor; (3) creation of a new type of online tool– a flood adaptation mapper; and (4) frequent incorporation of government and community stakeholder input. Follow-up studies are evaluating the influence of a range of flood mitigation scenarios on waves and water quality, studying how vegetation will co-evolve with protective measures and sea level rise, and quantifying other ecosystem service values beyond flood protection.

AdaptMap and the other products above are helping decision-makers and the general public visualize and quantify the benefits of natural features for reducing coastal flooding.

Table of Contents

1.0 Introduction

Coastal storms are among the world's most costly and deadly disasters, with strong winds, floodwater inundation, and coastal erosion capable of damaging and disabling infrastructure. Increased damage from storm surge flooding is one of the most certain impacts of climate change, with the potential for intensified storms, increased rainfall, and with storm surges coming on top of rising sea levels. Sea level rise is expected to accelerate over the 21st Century, primarily due to increasing expansion of warming seawater and accelerated melting of land-based ice sheets. A conservative estimate of 30-60cm for New York City (NYC) by 2080 will change a 100-year flood event to a 30-year flood event, and "rapid ice-melt" scenarios call for over a meter of sea level rise over this period [*Horton et al.*, 2010].

Hundreds of thousands of NYC residents in Jamaica Bay's watershed live on land within range of a 5 m hurricane storm tide (**Figure 1**), and Hurricane Sandy (3.5 m above mean sea level) flooded some of these neighborhoods. Hurricanes made direct hits on NYC four times over the last 400 years including 1693, 1788, 1821, and 1893 and will likely do so again [*Scileppi and Donnelly*, 2007]. Moreover, sea level rise of 1 m will mean that a severe extra-tropical storm (a "nor'easter") will lead to flooding levels nearly as bad as Sandy or the historic hurricanes – the worst nor'easters (e.g. 1992) have an annual probability of occurrence of one in twenty and cause maximum water levels of about 2.0-2.5 m [*Orton et al.*, 2012].

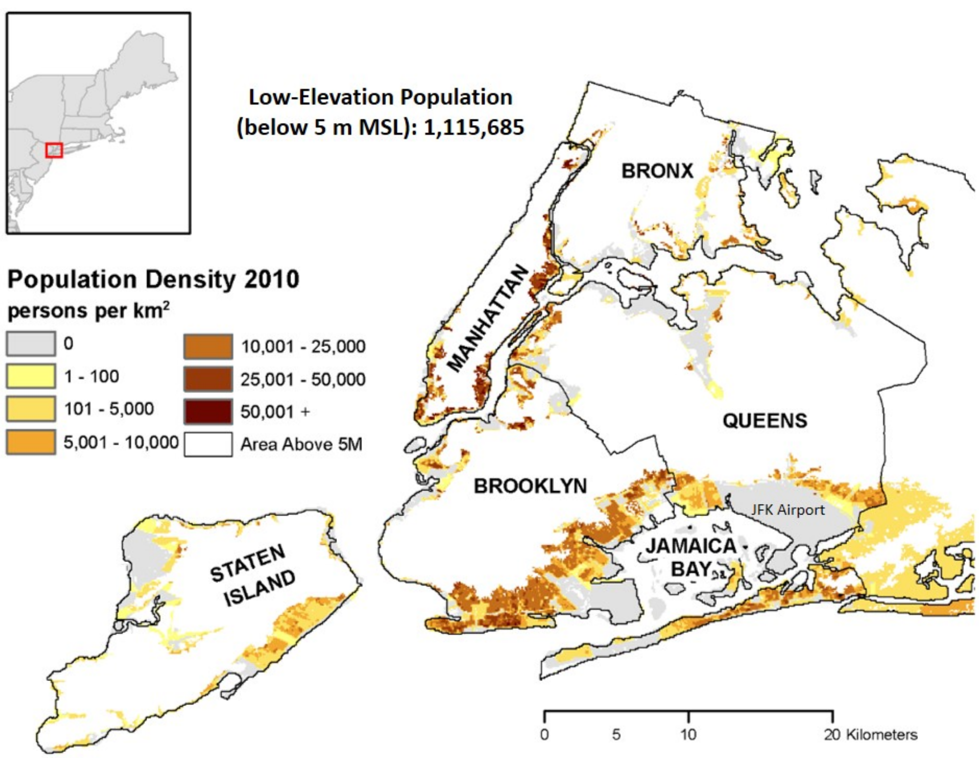

Figure 1: NYC map showing population and density in low-elevation coastal zones (LECZ) below 5 m above mean sea level. Hurricane Sandy's flooding was extensive in neighborhoods surrounding Jamaica Bay.

Before extensive dredging and reconfiguration of the Bay's entrance from 1912 to 1940, Jamaica Bay had a much shallower entrance channel and plentiful marshes. Shallow channels likely protected inland areas by attenuating storm surges – the system used to attenuate tides, whereas now tide ranges are amplified as tides flow from the entrance to the inner reaches of the bay [*Swanson and Wilson*, 2008]. Since then, the Bay's average depth has increased from 1 to 5 m, and the volume of the bay by 350% [*NYC-DEP*, 2007; *Swanson et al.*, 1992]. The total loss of interior wetlands since the mid-1800s is estimated to be 12000 of the original 16000 acre*s [NYC-DEP, 2007]*. A successful experimental Corps of Engineers program that has rebuilt a small portion of the tidal wetland islands in Jamaica Bay from 2009-2012 raises the possibility that these losses can be reversed (**Figure 2**), but the cost of rebuilding the losses from 1974-1999 alone has been estimated to be $310 million at ~$500/acre [S. Zahn, NY State Department of Environmental Conservation, pers. comm, 2012].

Figure 2: Small-scale Corps of Engineers marsh restoration efforts have had success in Jamaica Bay, and there is potential for expanding these efforts (Credit: U.S. Army Corps of Engineers).

Nationwide, natural coastal systems of many types are still disappearing, in spite of society's qualitative knowledge of their benefits. In recent decades, the decline of tidal wetlands has continued [*Dahl*, 2006]. Much like wetlands, shellfish reefs also can provide protective benefits from storm-driven waves and flooding, due to their rough surfaces and added frictional effect on rapidly moving waters. Unfortunately, wild oyster biomass in U.S. estuaries has declined by 88 percent over the past century [*Zu Ermgassen et al.*, 2012]. These changes are likely only partially a result of sea level rise – both wetlands and shellfish reefs are to a varying extent ecosystem engineers and can grow upward with sea level rise, though the maximum rates at which they can rise are uncertain.

Quantifying the economic values of these protective services for socioeconomic analyses is a crucial step for conserving these beneficial coastal systems [*NRC*, 2005]. NYC and many other municipalities across the nation are weighing restoration or protection of natural coastal systems, yet there is limited quantitative information available to help inform these decisions. An old rule of thumb holds that 14.5 km of wetlands reduces a storm surge by 1 meter, though this is based on an observational study of historical Louisiana hurricanes that actually showed variations of over a factor of three in the surge reductions [*USACE*, 1963]. More recent research has shown that the attenuation of storm surge by marshes actually varies even more than a factor of three, and wetlands sometimes do not attenuate storm surges at all. The attenuation by wetlands depends on many details including direction and duration of the storm's winds and waves, and the coastal topography and bathymetry around the wetlands [*Resio and Westerink*, 2008]. Our initial work prior to this project (e.g. City of New York, 2013; Orton et al. 2012) suggested that wetlands in the center of Jamaica Bay actually provide very little flood protection, and motivated this study to look more broadly at a wider range of coastal sedimentary and ecological systems for potential flood mitigation.

In this study, we have leveraged existing computational flood model-based flood zone mapping and risk assessments to quantify the value of various nature-based flood mitigation approaches, develop new nature-based concepts, and map their flood protection services. A case study of Jamaica Bay, New York City (NYC) has been utilized where the recent impacts of Hurricane Sandy have created strong public support for flood mitigation measures. Historical landscapes were mapped and their resilience to flooding studied, helping guide the development of novel nature-based flood mitigation measures. The work has helped to provide information and visualization needed to make decisions regarding the flood protections provided by nature-based features. This technical report lays out the methods, final highlighted flood adaptation scenarios, flood reduction results and a summary of the resulting online flood adaptation mapper, AdaptMap.

2.0 Methods

2.1 Jamaica Bay landscape reconstructions

For purposes of this study, we created three inter-comparable descriptions of the Jamaica Bay watershed, representing the contemporary conditions; the landscape in the 1870s; and the pre-European landscape of c. 1609, when Henry Hudson arrived off the shores of what would someday become New York City [*Sanderson*, 2009]. For each landscape we created a digital elevation model and a land cover map at 30 m resolution. The Jamaica Bay watershed describes approximately the area drained by the sewer systems feeding wastewater treatment plants today. It covers parts of Brooklyn and Queens, in New York City, and the Town of Hempstead, in Nassau Count, New York.

2.1.1 Present-Day Landscape

We extracted the recent ("present-day") land cover data for the Jamaica Bay watershed at 30 m resolution from the National Land Cover Dataset (2011) (NLCD) as described in Homer et al. (2015). At the request of our PAC (Project Advisory Committee), we evaluated the C-CAP data that is available, but found that urban classes of land cover that are dominant in our study area are not part of C-CAP.

The present-day topographic and bathymetric information was from a recent FEMA study [*FEMA*, 2014]. These data are a combination of bathymetric data from NOAA, which in itself is a mixture of data from different decades, and topographic data. It is noteworthy that these are not the latest (2010) LIDAR data, however. The model resolution for our flood simulations is 30 m and land elevations are taken from point samples within this higher-resolution topographic information. Therefore, the model does not resolve fine-scale features like elevated seawalls, though they are rare in this area.

2.1.2 Historical Landscapes

For the historical landscapes of the Jamaica Bay watershed, we synthesized historical maps and charts (e.g. **Figure 3**), accompanied with an intensive reading of the historical literature [notably, *Bellot*, 1917; *Black*, 1981; *Munsell*, 1882; *Ostrander*, 1894; *Stiles*, 1870; *Taney*, 1961]. Maps of the Brooklyn and Queens coastal environment were first made by Survey of the Coast of the United States (known later as the U.S. Coast and Geodetic Survey, and referred to for simplicity as the U.S. Coast Survey), which began its work in the New York City region in the 1830s [*Allen*, 1998; *Guthorn*, 1984]. Established in 1807, the Survey was the first U.S. scientific agency and is an ancestor of the modern National Oceanic and Atmospheric Administration in the U.S. Department of Commerce [*Shalowitz*, 1964]. In New York, the Survey produced printed chart series in the 1840s through to the early twentieth century; chart-making continues today with the familiar NOAA coastal charts. These maps have been frequently used for historical ecology studies [e.g., *Bromberg and Bertness*, 2005; *Grossinger et al.*, 2005].

We obtained high resolution scans of manuscript and printed charts from 1844 – 1907 with map scales ranging from 1:5,000 to 1:80,000. The U.S. Coastal Survey made topographic surveys of the shoreline and adjacent uplands, commonly referred to as T-sheets; and hydrological surveys of coastal waters, often with detailed bathymetric surveys, known as H-sheets. Of particular interest for our study were a pair of H-sheets from 1877 and 1878 of Jamaica Bay: Maynard [1877] and Moore [1878]. Maynard's survey was drawn at 1:5,000 scale, and Moore's survey at 1:10,000 scale. Both show grids of depth surveys, with parallel lines approximately 100 m apart, and with sounding data approximately every 20 m. They also include scattered observations of bottom condition including "sft" (soft), "hrd" (hard), "gy" (gray), "S" (sand), "M" (mud), and "Grass" (for eelgrass beds.) Moore [1878] includes depth contour lines that mark out channels between the marshy islands and other underwater features.

Figure 3: Maps of Jamaica Bay through the centuries (clockwise progression), showing the growth of islands and the Rockaway Peninsula in the 1700s and 1800s and growth of the peninsula but loss of islands in the 20th Century [*Sanderson*, 2016].

Graticules and clearly delineated locations on the maps for which modern location information were available were used to georeference the charts, typically using a first order rectification process. All maps were georeferenced with a less than 50 m root-mean-square error, as measured at the control points. We digitized the shorelines, extent of marsh, substrate material type, and all topographic and bathymetric information from H-sheets and other nautical charts. On T-sheets and other upland focused maps, we digitized topographic contours, point elevations, streams, ponds, forests, wetlands, built land uses, and other features. We also compiled toponyms from the maps for use correlating site descriptions in textual sources with the location of features in or around Jamaica Bay.

Because maps and charts were drawn at different times and sometimes with different definitions of shoreline (the "topographic zero", which might be defined relative to the observed mean sea level, mean lower low water or some other tidal datum), we adjusted elevations to a common vertical datum, in this case, NAVD88, adjusting for sea level rise. To do so we took advantage of the relative sea level reconstruction (RSL) provided by Kemp & Horton [2013]. Kemp & Horton [2013] studied foraminiferal assemblages over the past two centuries from salt marsh sediment in Barnegat Bay, New Jersey. Their results were used to identify RSL in the New York City region at the time the map or chart represents, and have been recently confirmed by analysis of a new core in Pelham Bay Park, in the Bronx (Kemp, pers. comm.)

To estimate the NAVD88 elevation of the topographic zero for each map, we noted that Kemp & Horton [2013] places the 0 level of their RSL reconstruction at 0.1 meter above mean sea level in Barnegat Bay. Mean sea level today for their study site was determined using NOAA Tides & Currents adjustment values for Barnegat Inlet [Station 8533615; *NOAA*, 2015]. We also used the seaward and landward extents of the salt marshes around Jamaica Bay as sources of elevation information. The seaward extent of salt marsh indications were assumed to represent the mean sea level (the lower edge of the low salt marsh, Edinger et al. [2014] and the landward edge to represent the extent of highest tidal flooding [the upper edge of the high salt marsh, *Edinger*, 2014]. A few maps provide an indication between low and high salt marsh, which was associated with the mean high tide. Historic tidal ranges were drawn from observations made at Governors Island and recorded on Hassler [1844].

Raster digital elevation models (DEM) were created in ArcGIS 10.3 with the "Topo to Raster" tool. This special interpolation method was devised to create hydrologically correct DEMs [*ESRI*, 2016]. In addition to contour line and point elevation data, historical stream and pond data were also added. To preserve the winding characteristics of marsh creeks during the interpolation, creek beds were converted to point features and their elevation was set at the Mean Lowest Low Water level of 1609. Finally, historical salt marshes were included in the interpolation, but required separate treatment because of the relatively small elevation change across the marsh surface. Within salt marshes, values between upper boundaries (MHHW) and lower boundaries (MSL) were interpolated using Topo to Raster. The resulting marsh-derived DEM was then clipped to the historical wetland extent and converted to a point feature for use as input in the final model.

For the c. 1870s digital elevation model, we used a combination of several high-resolution H-sheet and T-sheet manuscript maps to construct a high resolution DEM. While earlier H-sheets depicted the bathymetry of Rockaway Inlet and Broad Channel, the Maynard [1877] and Moore [1878] manuscript maps are the first to depict the bathymetry of the entirety of Jamaica Bay. Approximately 20,000 individual sounding points were digitized to describe the interior of the bay, and were paired with contour lines and specific elevation points derived from Bien and Vermule [1891b], Bien and Vermeule [1891a], Dorr [1860], Gilbert [1855a], Gilbert [1856a], Gilbert [1856b], Gilbert and Sullivan [1857], Powell [1891], and Wilson [1897]. This topographic information extends outside of the study area to describe the topography of Long Island south of the terminal moraine.

For the c. 1870s land cover map, we mainly used digitized features from the Bache [1882] coast chart. The Bache chart represents a synthesis of several T-sheet and H-sheet manuscript maps that were created during the period of 1866-1882. This chart depicts salt marsh, agricultural land, towns, beaches, scrubland, upland forests, and emergent coastal forests at a scale of 1:80,000 and was digitized at a scale of 1:3,000. Unfortunately the Bache [1882] chart doesn't show the easternmost part of the bay, so we used two manuscript maps by Jenkins [1837a; b] for that area. The landcover indications on these maps were interpreted to match landcover classes described by the 2011 National Land Cover Dataset [*Homer et al.*, 2015] for comparison to other scenarios in this study.

For the c. 1609 digital elevation model, we used a combination of U.S. Coast Survey charts, Revolutionary War-era maps, and early-mid 19th century municipal planning maps to create an elevation profile for the Jamaica Bay watershed. We selected features that were not obviously changed by human activity and all from maps prior to major urban development. Topographic contour lines and specific elevation points were digitized from Anonymous [1783], Bien and Vermule [1891b], Dorr [1859], Dorr [1860], Eddy [1811], Gilbert [1855a; b; 1856a; b], Gilbert and Sullivan [1857], Hassler [1844], Powell [1891], Rockwell and Whiting [1858], Whiting [1850; 1862] and Wilson [1897]. These elevation data were used to generate a composite elevation model depicting the study area in 1609. The absence of interior marsh islands and Rockaway Peninsula barrier island are discussed in Sanderson [2016].

A particular problem for the 1609 landscape was the historic location of the Rockaway Peninsula and the interior marsh islands in Jamaica Bay. Comparative study of US Coast Survey charts in the late 19th c. shows considerable movement of the Rockaways, on the order of 0.5 – 1.5 cubic meters of sand per meter of beach front per year (**Figure 4**). This motion was sufficient to extend the Rockaway Peninsula westward on average 77 meters per year between 1844-1907 [*Giampieri and Sanderson*, in preparation; *Swanson et al.*, 2016] ; [see charts by *Bache*, 1861; 1882; *Bien and Vermeule*, 1891b; *Hassler*, 1844; *Tittman*, 1907]. To attempt to fix more exactly the 17th century location of the Rockaways, we compared and contrasted a set of 100 maps and charts from 1501 – 1844. Although these historical maps drawn from Dutch, English, French, Swedish and American sources require careful interpretation and appreciation for historical context, in series they appear to suggest that Jamaica Bay was formerly much more open, without the interior marsh islands [*Sanderson*, 2016]. From these observations, we formed a hypothesis regarding the east to west extension of the Rockaway Peninsula that in turn led to salt marsh formation in the interior of the bay approximately 200-230 years ago.

For the purposes of the 1609 digital elevation model and land cover map, these studies result in an interpretation that excludes any interior Jamaica Bay marsh islands and shows a truncated, and largely-sub-surface, form of the Rockaway Peninsula, much as described in Robert Juet's journal from the Henry Hudson expedition [*Purchas*, 1625]:

At three of the clocke in the after-noone [on September 3, 1609], wee came to three great Riuers. We stood along to the Northermost, thinking to haue gone into it, but we found it to haue a very shoald barre before it, for we had but ten foot water.

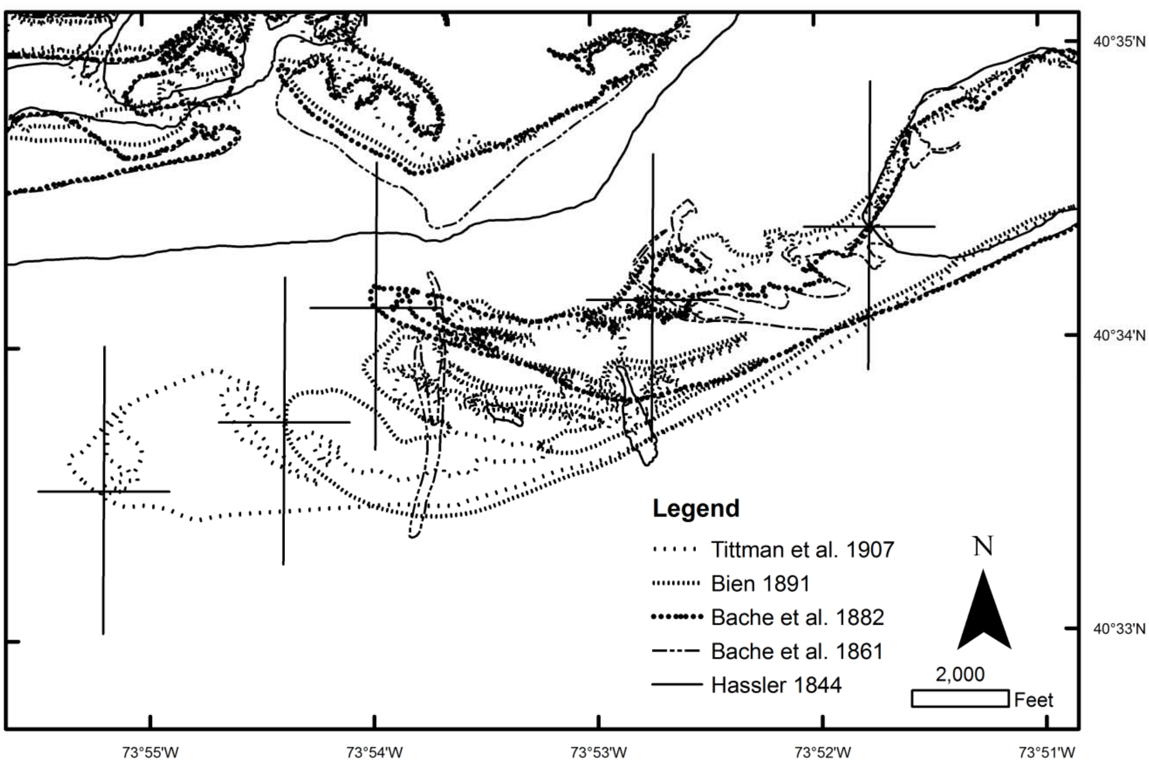

Figure 4: Historical map-based progression of the tip of Rockaway Peninsula over time, 1844 to 1907 [*Giampieri and Sanderson*, in preparation; *Swanson et al.*, 2016].

The 1609 location of the Rockaway peninsula, Barren Island, the topographic synthesis and the near shore- and bay bathmetry should all be considered speculative, but the best we can do given the currently available data [*Sanderson*, 2016]. Future studies could use morphodynamic computer modeling to develop a more detailed possible bathymetric map for the area, capturing realistic sandbars, tidal channels, and other features.

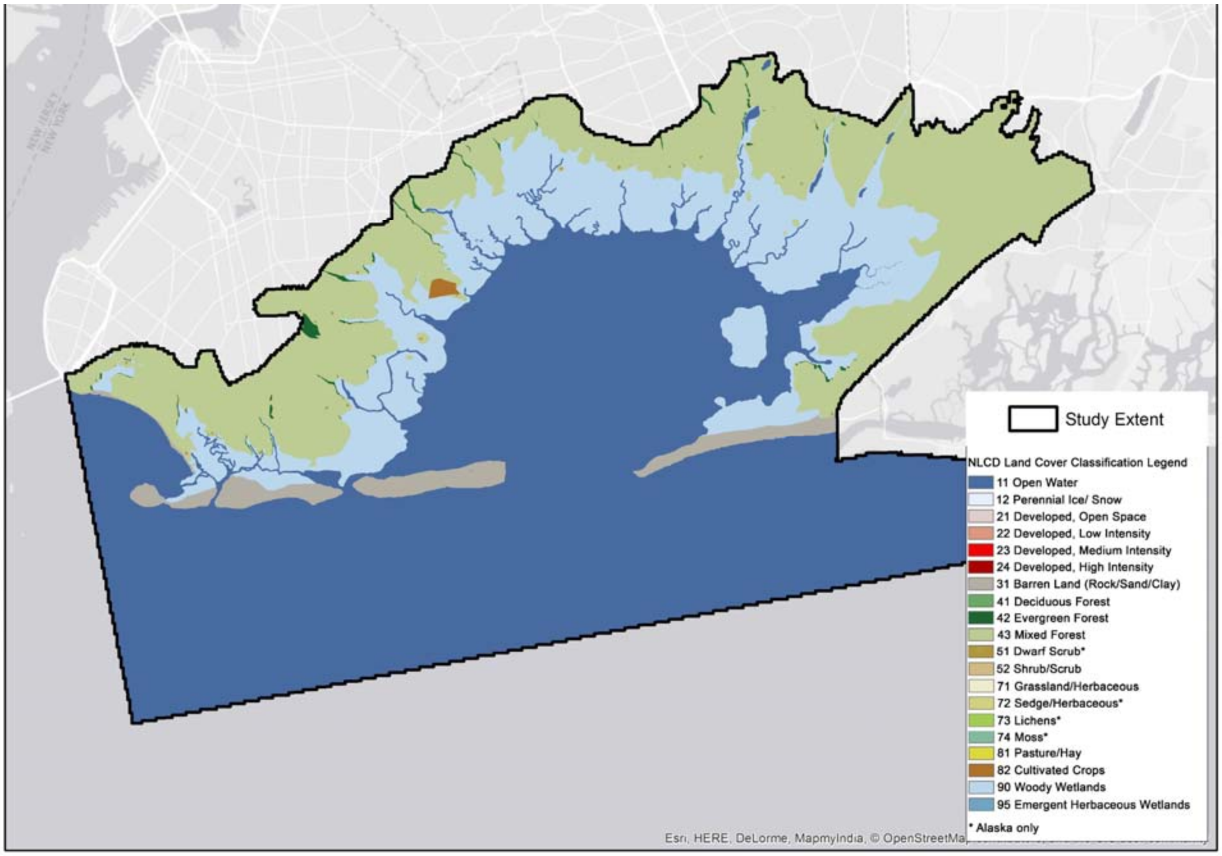

Figure 5: Reconstructed land cover of the Jamaica Bay watershed, c. 1609.

Similarly the c. 1609 land cover is of necessity somewhat speculative, though here we can use known ecological relationships to help reinforce our interpretation of the pre-development ecology [*Sanderson*, 2009; *Sanderson and Brown*, 2007]. The upland was largely forested, as we can see by observing in 19th century maps, the agricultural landcover of the Jamaica Bay watershed, with large remnants of remaining forest [for example, on *Hassler*, 1844]. For the c. 1609 land cover map, we used an elevation-based modeling approach to derive landcover classifications, again adhering to the NLCD typology, for the study area. Areas above the highest tidal influence were classified as mixed deciduous forest; intertidal areas around Jamaica Bay that have been historically depicted as salt marsh zones were classified as emergent herbaceous wetlands [*Sanderson*, 2016]; and seaward intertidal areas were depicted as mudflat and estuary waters. Land cover classes continue to be refined through the Welikia Project (welikia.org).

Final maps of estimated Jamaica Bay area land cover for the present-day, 1877 and 1609 periods are shown in **Figures 5, 6 and 7**. Land elevations (topography, bathymetry) are shown in **Figure 8, left panels**.

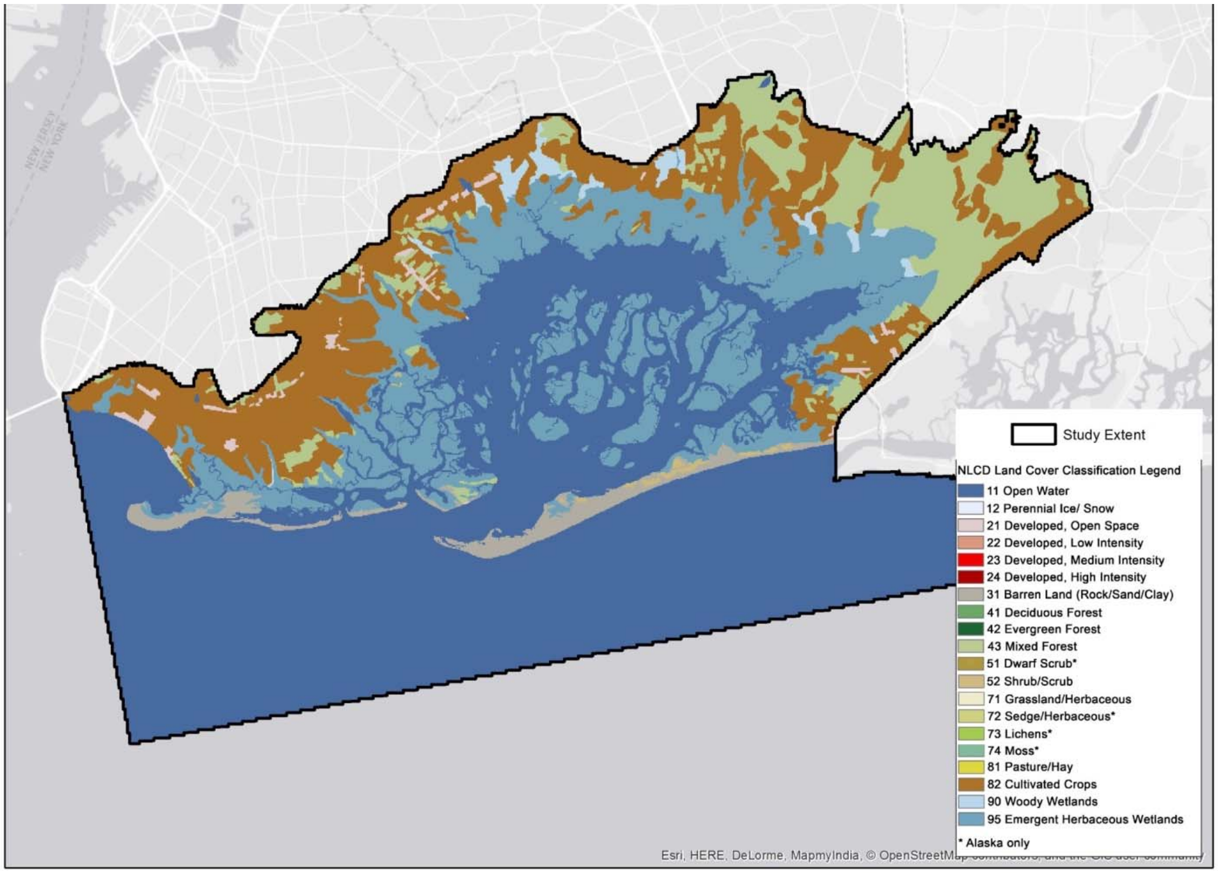

Figure 6: Reconstructed land cover of the Jamaica Bay watershed, c. 1877.

2.2 Hydrodynamic modeling

A validated hydrodynamic model and model grid is used in the study to simulate the storm tides. The hydrodynamic model sECOM provides highly accurate 3D storm tide predictions as part of the NY Harbor Observation and Prediction System (NYHOPS)[*Georgas et al.*, 2014; *Orton et al.*, 2012]. The model grid is a 30 by 30 meter, square-cell grid. Simulations for this study use the models' two-dimensional (2D) mode, and are doubly-nested inside larger model domains. More detail can be found in Orton et al. [2015].

Gridded land elevation and land cover type datasets were constructed for the historical and potential future mitigation landscapes. These were used to create 1609, 1877 and present-day model grids for sECOM (see **Section 2.1**), including land elevation and Mannings-n roughness (**Figure 8**). In 2D storm surge modeling studies, a common simplified approach to representing the effects of wetlands and other natural features is to treat them as enhanced landscape roughness features, through a variable called Mannings-*n* [*Orton et al.*, 2015]. Mannings-*n* values for wetlands are 0.045, and those for other common land-cover types in the model are: 0.02 for open water, 0.09 for barren land (rock, sand or clay), and 0.10 and 0.13 for medium and high intensity developed land, respectively.

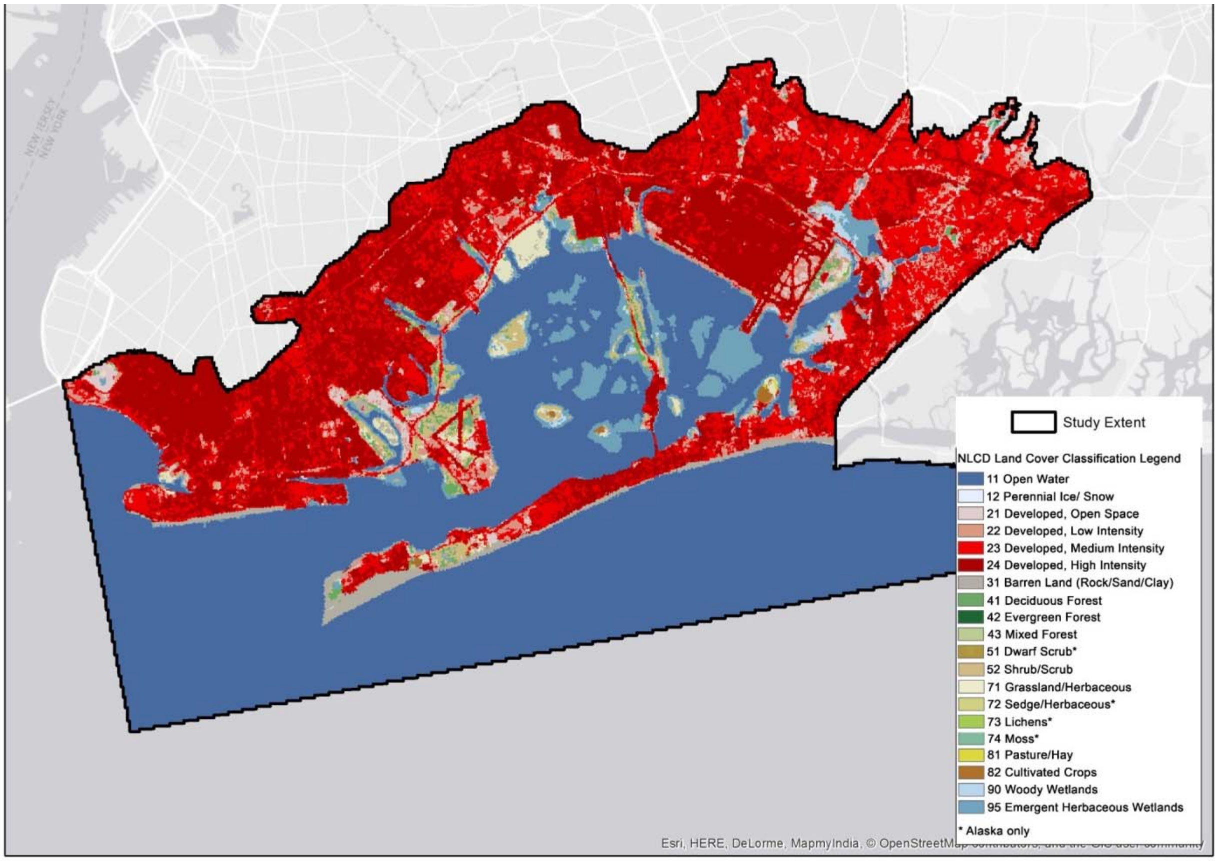

Figure 7: Land cover distribution of the Jamaica Bay watershed, 2011. Based on the National Land Cover Dataset [*Homer et al.*, 2015]

2.3 Flood mitigation measure testing and development

Experimentation on possible flood mitigation scenarios began with "leverage experiments", flood modeling experiments designed with simplistic landscape or land cover changes, to coarsely evaluate the potential for a scenario to reduce flooding. These experiments are useful for brainstorming and quickly evaluating the potential for various types of flood adaptation. The initial work under this project demonstrated that inlet or estuary channel depth shallowing can be used to reduce or even prevent coastal flooding in this area, whereas massive wetland restoration in the center of the bay was not effective for reducing flooding [*Orton et al.*, 2015].

A flood mitigation workshop was held in May 2015 with government agency representatives, urban planners, designers, scientists, and the general public, to take input on an initial set of mitigation concepts and allow for new ideas to be contributed. Subsequently, a broader series of leverage experiments was performed over several months to quantify potential flood reductions from a wider range of adaptation scenarios that could be applied to the modern-day landscape.

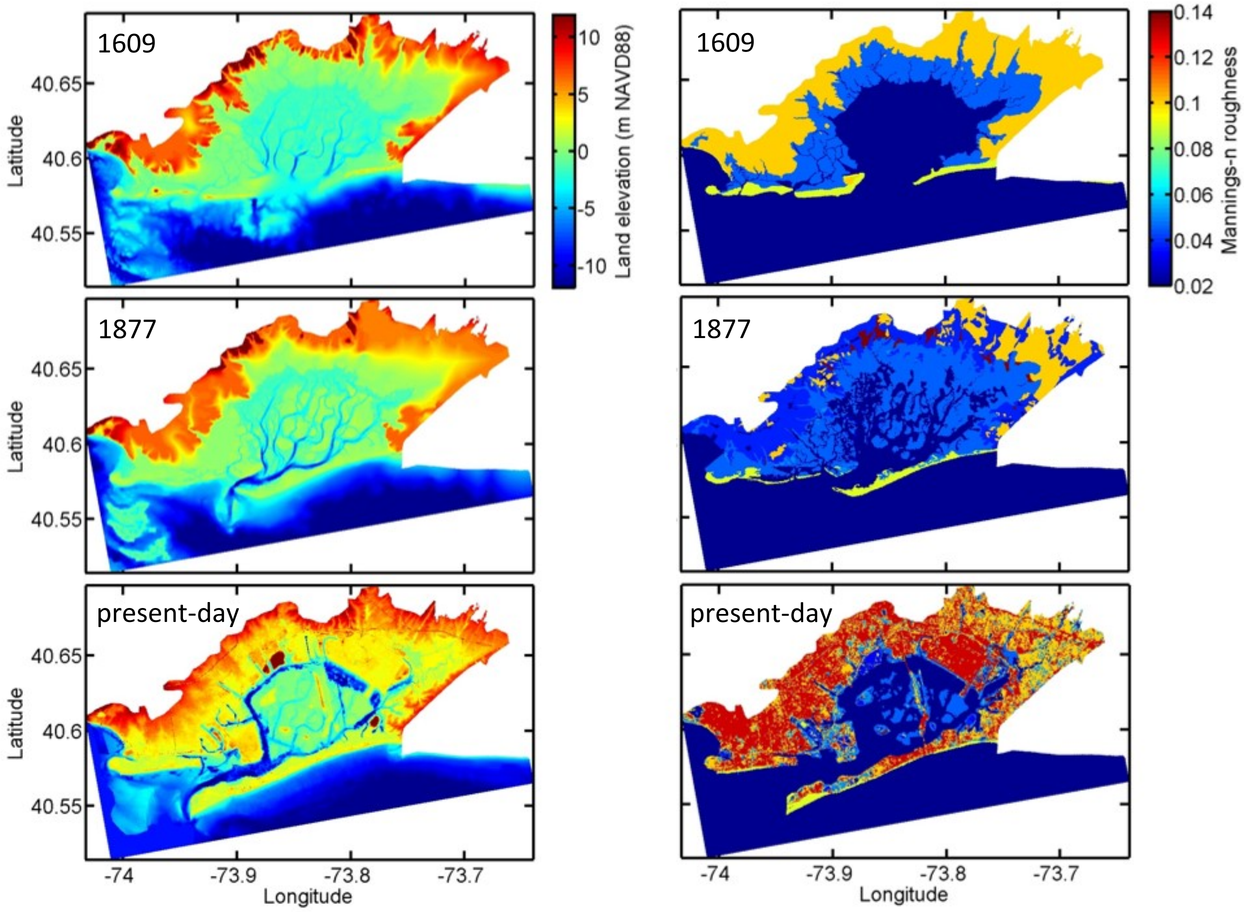

Figure 8: Historical and present-day landscape data used as inputs to the hydrodynamic model – on the **left** are land elevation maps, and on the **right** are land-cover roughness (Mannings-n) maps. The **top row** shows 1609, the **middle row** shows 1877, and the **bottom row** shows the present-day landscape. The 1609 landscape bathymetry is unknown, and thus prone to error, whereas the 1877 bathymetry is taken directly from detailed survey maps. The presence of "grass" (likely eel grass) on the 1877 bed was mapped and is included in the Mannings-n data. The absence or presence of eel grass in 1609 is not known. In this study, it was assumed absent, but it is likely there was eel grass and other roughness elements (e.g. oysters) in the bay at that time.

Scenarios that were tested for their efficacy in reducing flooding included:

- fringing wetland restoration
- central bay wetland restoration
- offshore shoal creation
- channel shallowing
- bay roughening
- inlet narrowing
- oyster reef creation

- new inlet creation
- replacement of garbage landfill sites with wetlands
- replacement of neighborhoods with wetlands through buy-out programs

In total, 44 specific landscape scenarios were evaluated for their impact on flooding from the Category-3 hurricane of 1821 [e.g., *Orton et al.*, 2015]. In a separate report, we summarized the scenarios, the flood reduction results, display a few representative scenarios and interpret the physical reasons for changes in flood elevations [*Orton and Wu*, 2015].

The leverage experiments showed that the most effective flood mitigation options, by far, involved actions at the inlet. Shallowing the inlet can reduce the inland penetration of a coastal flood through enhancing frictional effects on the water flow, slowing water speeds and the rate at which the bay fills with water. Narrowing the inlet can similarly "choke" flow into the bay and reduce flood elevations by reducing the amount of water that gets into the bay. Shallowing within the bay is also effective to some extent, as it reduces the speeds that water rushes through the channels that run around the bay interior [*Orton et al.*, 2015].

The inlet's cross-sectional area reaches a minimum off Floyd Bennett Field, a reduction of 33% from 15000 to 10000 m^2, for a 2 m storm tide event [Orton and Wu, 2015], and this has the potential to choke flows into the bay, serving as a sort-of bottleneck. Further choking the flow by narrowing the channel at Floyd Bennett Field was found to have a strong leverage on storm tides in the bay, yet also caused reflection and new flooding at points outside the bay. A new area of narrowing off eastern Coney Island (by Kingsborough Community College) was tested and found to mitigate this problem. Subsequent flood mitigation scenarios included both narrowing off Coney Island and at Floyd Bennett Field.

A set of three recommended scenarios was developed based on the public input and the results of the leverage experiments, for evaluation with a full flood hazard assessment and benefit-cost analysis, and for display on the project's webtool, AdaptMap. These were released for a last round of input from the Project Advisory Committee, and finalized in fall 2015.

2.4 Coastal flood hazard assessment and changing sea levels

A flood hazard assessment is a study that quantifies the annual probabilities of any given flood height occurring. Here, we use a method of flood hazard assessment that is an ensemble computer simulation of a full set of possible storms (storm climatology) ranging from tropical cyclones (hurricanes) to extratropical cyclones (e.g. nor'easters). There has been a wide range of results in prior NY Harbor area studies, with the 100-year storm tide being defined by FEMA as 3.5 m and by [*Aerts et al.*, 2014] as 2.03 m. Our assessment methods are validated by comparison to historical data at multiple levels of the study, aiming to improve confidence in our understanding of the region's potential for flooding. A recent submitted paper summarizes the methods including details of historical data, validations, storm climatology development, and statistical analysis [*Orton et al.*, submitted].

Results from the aforementioned flood hazard study for NY Harbor are used as offshore boundary data for our Jamaica Bay model grid. That study included 1516 storm simulations, but here an abbreviated storm set is used here, including 64 tropical cyclones and 80 extratropical cyclones. For the present-day sea level and control model grid, a comparison was made of the results using an abbreviated versus full storm set, and differences were below 3% for the 5-year to 1000-year storm tide results. The same methods are used for historical cases (1877 and 1609) and future cases, simply by simulating the storms on the model grid for that year or for each flood mitigation landscape.

Sea level varied historically and will rise through the coming century, and different sea levels are applied to the hazard assessment by raising or lowering the initial sea level at the grid's offshore boundary for each model run. The sea level in this study for 1877 of -0.28 m (-11 inches) was taken from *Kemp and Horton* [2013], whereas the 1609 sea level estimate of -0.61 m (-24 inches) required a projection back in time from 1788 (-0.49 m) to 1609 using an assumed land elevation change from that study of 0.66 mm y^{-1} (0.12 m lower), also from *Kemp and Horton* [2013]. These are the same mean sea level estimates used for converting map datums (e.g. from mean lower-low water to navd88) for the bathymetry, so are self-consistent. Future sea level projections for 2055 from the New York City Panel on Climate Change are low-end 10^{th} percentile, median 50^{th} percentile, and high-end 90^{th} percentile estimates [*Horton et al.*, 2015] of 24 cm (10 inches), 45 cm (18 inches) and 80 cm (32 inches) after adjustment so they are relative to the 1983-2001 mean sea level datum. Present-day 2016 sea level is an estimate of +10 cm (4 inches) over that datum, based on an estimated 4 mm/y sea level rise rate inferred from the historical data at New York City (The Battery, a NOAA tide gauge).

Uncertainty in the flood hazard was quantified in the prior New York Harbor study for the zero sea level rise case (present-day) [*Orton et al.*, submitted]. Here, those uncertainties are applied statically on top of the flood hazard for the future sea level rise scenarios, and assumed to be the same and constant across Jamaica Bay (the flood exceedance curves at NY Harbor and Jamaica Bay are very similar). The Monte Carlo uncertainty methods from the NY Harbor study were adjusted from 95% confidence to 80% confidence intervals, to match the NPCC sea level rise estimates. These storm tide uncertainties (in meters) were fitted with a third-order polynomial curve (versus return period) for application onto different future flood exceedance curves. To provide a complete uncertainty for the future 2055 scenarios, 1000 Monte Carlo ensembles of storm tide and sea level rise were then merged, to preserve the distributions of uncertainty (no assumption of normally-distributed uncertainty).

2.5 Damage assessment

Damage assessments for the full array of landscape, sea level, and storm tide scenarios (including uncertainty) were estimated using FEMA's HAZUS-MH software supplemented with User Defined Facilities (UDF) data. The estimates were then transformed using an adjustment factor derived from several independent estimates of flood-related damages in the study area following Hurricanes Irene and Sandy.

2.5.1 User Defined Facilities

UDF data at the building level were obtained from FEMA's CommunityViz project for New York City. Using these data, the HAZUS-MH Flood methodologies damage estimation procedure was automated in Python to produce building and contents damage estimates for the entire set of inundation scenarios (5-year to 10000-year floods).

2.5.2 Critical Infrastructure

The geographic database of critical infrastructure produced in this work consists of a variety of structures at risk from flood events including:

- Fire stations
- Police stations
- Hospitals
- Schools
- Community service centers
- Power plants
- Wastewater treatment plants
- Roads
- Subway/rail stations
- MTA bus depots

2.5.3 Adjustment of Damage Estimates

Damage estimates produced through a HAZUS-MH assessment of flood grids of Hurricanes Irene and Sandy from the FEMA Modeling Task Force [*FEMA*, 2013] were compared to estimated real-world damages. The HAZUS-MH Flood model provides damage estimates for buildings and their contents, but we use observed damages from Irene and Sandy to create scaling factors that modify our damage estimates in order to capture all flood related damages, including indirect economic impacts and infrastructure damage [e.g., *Aerts et al.*, 2014].

To get an estimate of the portion of total NYC damages in Jamaica Bay caused by Hurricane Sandy, five spatially disaggregated damage data sets [*FEMA*, 2013; *Sandy Funding Tracker*, 2016a; b; *US-HUD*, 2013; *US-SBA*, 2012] were referenced. Each of these contained estimates for some portion of total flood related damages, but the compendium was needed to get a complete and total estimate, and to quantify uncertainties. These combined estimates enabled the derivation of the proportion of damages contributed to the total for NYC by the portions of Kings, Queens, and Nassau counties contained by the Jamaica Bay study area. By using this method, central estimates and upper- and lower-bounds for the fraction of damages in Jamaica Bay were obtained. Finally, the central estimate, as well as the low and high end uncertainty estimates, was multiplied by a widely cited damage cost estimate from Hurricane Sandy for NYC as a whole, $19 billion [*Gormley*, 2012], to provide a final range of damages.

To get an estimate of the flood related damages in the Jamaica Bay study area attributable to Hurricane Irene, a different method was used. A methodology outlined in the Irene Tropical Cyclone Report [*Avila and Cangialosi*, 2011] and data on insured loss estimates from Insurance

News Net [*Jeffries*, 2011] were used to derive a set of three damage estimates. These estimates were then combined with a fourth from NOAA [*NOAA-NCDC*, 2011] to produce a final damage estimate and uncertainty range for the whole of the USA. Next, the proportion of damages in the Jamaica Bay study area were derived using the fraction of total verified loss in Jamaica Bay from the US-SBA [2011], which was then multiplied by the final damage estimate range.

Final damage estimate ranges:
Sandy: $12.7 billion ($9.8 – $15.6)
Irene: $93.7 million ($66.3 – $121)

The two damage estimate ranges were finally used to adjust the initial damage estimates and to construct an 80% confidence interval.

Table 1: The adjustment factors used for each return period.

Return Period	Adjustment factor (low)	Adjustment factor (mid)	Adjustment factor (high)
5	0.11	0.156	0.202
10	0.11	0.156	0.202
30	0.161	0.221	0.281
50	0.287	0.384	0.48
100	0.603	0.791	0.978
300	1.868	2.418	2.968
500	1.868	2.418	2.968
1000	1.868	2.418	2.968
10000	1.868	2.418	2.968

Prior studies have shown that adjustment factors need to be used to modify the HAZUS results so that they accurately estimate total monetary damages, which can overestimate damages from small floods [pers. comm., Hans de Moel, 04/2016, VU University] or underestimate damages due to not including all types of damage [e.g., Aerts et al., 2014]. The ratio of indirect to direct damages has been shown to be higher for longer return period floods [*Koks et al.*, 2015], which supports our increasing adjustment factor shown in **Table 1**.

To calculate an adjustment factor for each return period from 5-year to 10000-year (**Table 1**), it was first necessary to determine the effective return periods for Hurricanes Irene and Sandy in Jamaica Bay. This was accomplished through the use of damage estimates from the automated HAZUS procedure described above, and assuming a linear relationship between return period and damages (accurate for small changes in return period). For Hurricane Irene it was calculated as a 22-year return period event, and Hurricane Sandy was determined to be a 300-

year event. The adjustment factor from Hurricane Irene was used for events with return periods less than 22, and the adjustment factor from Hurricane Sandy for the storms with return periods greater than 300. For storms with return periods between 22 and 300, a linear relationship between return period and adjustment factor were assumed, and values were interpolated between the two end points (**Table 1**). The number of buildings and facilities impacted by each flood scenario were estimated by intersecting flood inundation layers with UDF critical infrastructure data.

2.6 Benefit-cost analysis

Numerical integration of adjusted losses over all return periods for each sea level scenario yields an expected annual damage (EAD) for each landscape and sea level combination [*Olsen et al.*, 2015].

$$EAD = \frac{1}{2}\sum_{i=1}^{n}\left(\frac{1}{T_i} - \frac{1}{T_{i+1}}\right)(D_i + D_{i+1})$$

Here T denotes return period and D denotes damage.

The EAD of each adaptation landscape scenario was subtracted from that of the present day landscape to derive the expected annual benefit (EAB) of implementing a given adaptation. This computation was performed for the 2016 central estimate and upper-bound and lower-bound estimates of the EAB, then also for the same for 2055. A linear relationship between the EAB and time was assumed, with values interpolated between 2016 and 2055 sea level scenarios. The adaptations were assumed to be built immediately. The discount rates (3%, 5%, and 7%) were then applied to the EAB for each year to provide a range of estimates.

$$B = \sum_{t=0}^{39}\frac{EAB_t}{(1+d)^t}$$

Here B denotes benefit, d denotes discount rate, and t denotes the time past 2016. Uncertainties from the flood hazard/sea level rise estimates, as well as the adjustment factors (**Table 1**), were merged to produce a final 80% confidence lower- and upper-bounds of the Benefit for each landscape scenario.

3.0 Results

3.1 Flooding for 1877 versus present-day landscapes

The flood hazard assessment reveals the flood area and water elevations for storms at various return periods, including the 100-year flood. The 100-year flood on the present-day landscape in Jamaica Bay is about 2.9 m (**Figure 9**, left panel). An important finding that informed the flood mitigation scenario development was that the 1877 landscape attenuates the water elevation for this 100-year flood, and flood elevations decrease with distance into the bay. The 100-year flood elevation declines from 2.8 m offshore to 2.3 m in the northern parts of the bay (**Figure 9**, right panel). The flood area, however, is larger, due to the low-lying floodplain that surrounded the bay which has been landfilled and is now airports and neighborhoods.

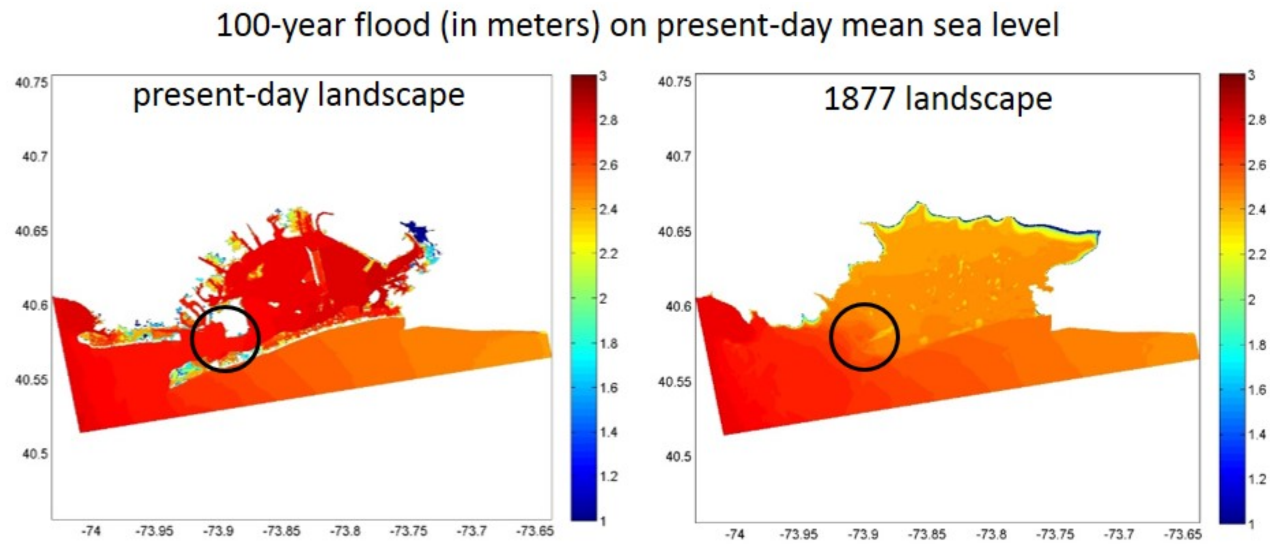

Figure 9: Maps of the 100-year flood (storm tide) from the full hazard assessment, for the present-day and 1877 landscapes. For both cases, storm tides were simulated on the present-day mean sea level, to capture effects of the difference landscapes on the same flood events. A circle around the location of the inlet highlights the strong attenuation of storm tide entering the bay.

3.2 Flood mitigation scenarios

Two of the three flood mitigation scenarios for full assessment are shown in **Figure 10**, and the three are described one-by-one below. In order to help users of AdaptMap understand the specific impacts of each part of each measure, the three scenarios are cumulative. That is, scenario #2 includes the changes in #1, plus additional changes. And scenario #3 includes the changes in #2, plus additional changes. This was one of many stakeholder suggestions that were incorporated into the project.

The three mitigation strategies aim to partially or completely reverse the effects of extreme over-dredging and widening of the bay's channels in the early 1900s. As shown in the prior section, in the 1800s the bay had a narrower, shallower inlet that choked floodwater flow into the bay and helped reduce flood elevations in the bay (**Figure 9**). Today's bay provides no protection due to the 8-16 m deep and 1 km wide Rockaway Inlet (at Floyd Bennett Field).

1) Inlet narrowing: This flood mitigation strategy simply narrows the inlet, seeking to reduce the rush of water into the bay during a storm surge. There would be a "sand engine", living shoreline or breakwater/reefs to narrow the Rockaway Inlet off eastern Coney Island (by Kingsborough Community College), and (2) sand or living shorelines to narrow the inlet off Floyd Bennett Field.

2) Narrowing and Sand Replenishment: This adaptation scenario would include (1) the two inlet narrowing strategies cited above, and also (2) a bay-wide shallowing (to 6.8 m maximum depth, which is 20 ft depth below normal low tide), and (3) channel roughening (increased sand waves, oysters, mussels, clams, shells). The inlet would still be very wide, so the narrowing should have no effect on shipping. The channel roughening is assumed to occur for any of multiple reasons – either due to mined sand from offshore having shell fragments, infill intentionally being mixed with fragments, or due to natural sand waves forming after shallowing, due to the increased water velocities that would occur. The influence of the roughening is relatively minor compared with the narrowing and shallowing.

These changes could reduce circulation and water quality in the bay, unless other major changes were made to mitigate these effects. Tide simulations (not shown) reveal a small reduction in tide range (18%). This may reduce flushing of bay, but also may help wetlands survive, as some hypothesize that growth in tide ranges since the 1800s is at least partially responsible for the wetland loss [*Swanson and Wilson*, 2008]. The water quality topic is being evaluated with further study (see **Section 4.5**). Addition of sand to bay may help ecosystems and wetlands, which presently may be starved of inorganic sediments they need as stable substrate.

3) Shallows Restoration – This is a strategy that builds upon the changes in Channel Repair by also tapering the shallowing of depths with distance eastward into the bay, with a secondary goal of restoring the natural sedimentary system of the bay. This approach leads to ~60 cm flood elevation reductions for the 100-year flood.

The above mitigation scenarios are given to the hydrodynamic model through two input datasets – the land elevation data (comprising topography, bathymetry), and the land roughness data, where land cover types are converted to Mannings-n roughness numbers (see **Section 2.2**).

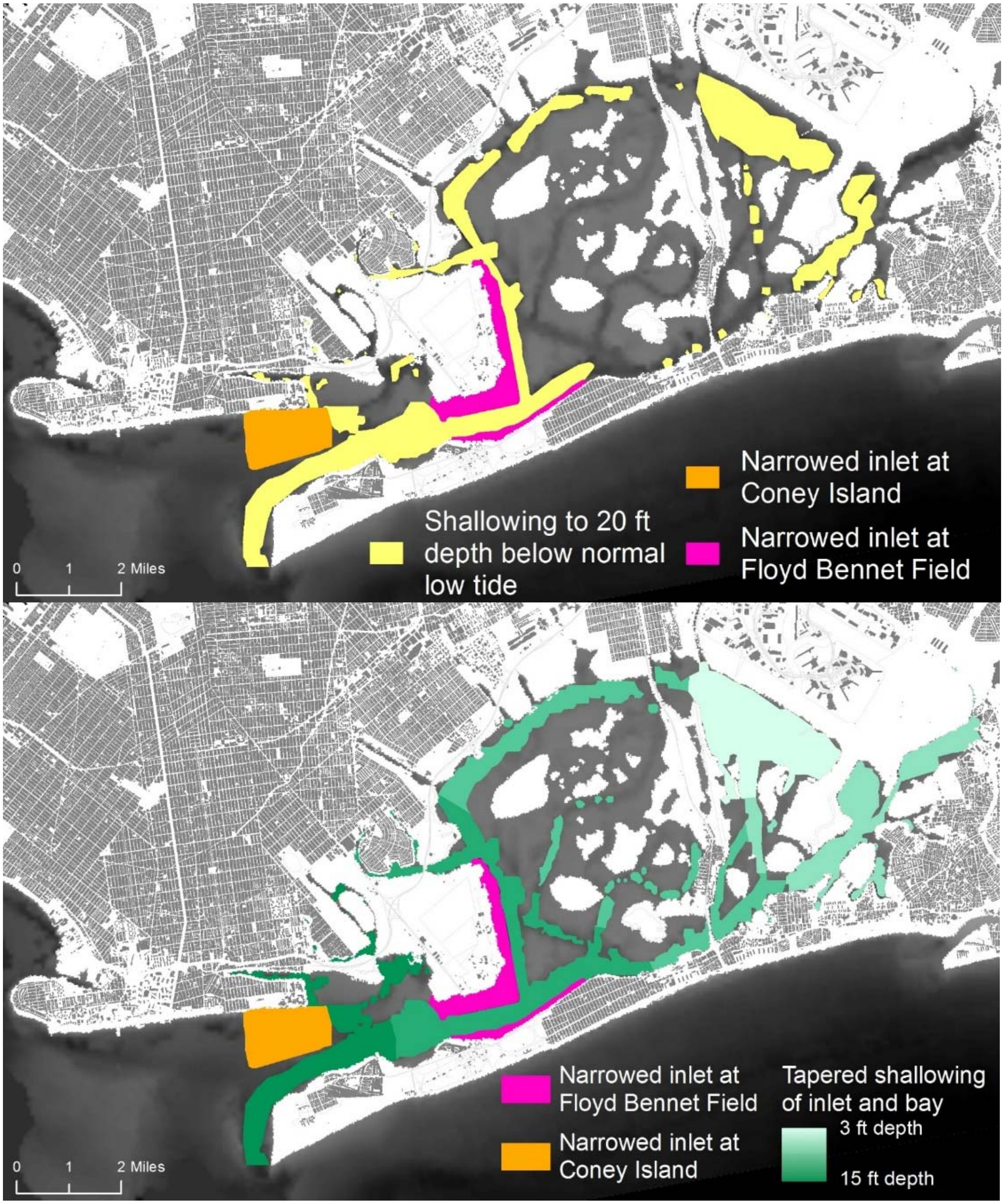

Figure 10: Maps illustrating flood mitigation scenarios #2 (top) and #3 (bottom). Scenario 2 includes inlet narrowing and sand replenishment (inlet/channel shallowing). Scenario 3 also the same, but has a more extreme, tapered shallowing with distance into the bay. Scenario #1 is not pictured, as it is captured in the map of #2 (it includes only the inlet narrowing features).

3.3 Impacts of mitigation scenarios on flooding

The flood elevations and area for the full range of flood events from the 5-year to the 1000-year storm are quantified with our analysis, for each landscape scenario. Differences between the control (present-day) landscape scenario and the flood mitigation scenario lead to both a reduction in flood elevation (**Table 2**) and area (**Tables 3-4**). For Scenarios #2 and #3 these are mapped in **Figures 11 and 12**. Scenario #1 has relatively minor impacts, so is not shown (however, results are available in AdaptMap).

Results for Scenario #2 are particularly noteworthy for the fact that nearly all flooding of neighborhoods is prevented for the 10-year flood (**Figure 11**, top panel) – a reduction in flooding of 98% for areas above 1.8 m NAVD88 (**Table 4**). The reduction in flood elevation in the bay is 17-19 cm (**Table 2**), and the reduction in flood area is 8.7 km^2 (**Table 3**).

Likewise, Scenario #3 prevents virtually all upland flooding (97%) for the 10-year flood (**Table 4**). Neither scenario is successful at preventing all flooding for the 100-year flood, but #2 reduces flood levels by 36-38 cm (**Table 2**), flood area by 10.1 km^2 (**Table 3**), and upland flood area by 62% (**Table 4**). Scenario #3 reduces the 100-year flood elevation by 62-67 cm, the flood area by 12.1 km^2 and the upland flood area by 73%.

Table 2: Flood levels (m navd88) for various return periods, locations, and mitigation scenarios

		10-year		100-year		1000-year	
Location	**Scenario**	**2016**	**2055[a]**	**2016**	**2055[a]**	**2016**	**2055[a]**
Eastern Bay (Inwood)	**Control**	2.08	2.39	2.72	3.15	4.15	4.43
	Scenario 1	2.00	2.37	2.56	2.93	3.94	4.23
	Scenario 2	1.89	2.22	2.34	2.74	3.69	4.04
	Scenario 3	1.68	2.03	2.10	2.52	3.36	3.77
Northern Bay (Spring Creek Park)	**Control**	2.04	2.38	2.67	3.07	4.08	4.36
	Scenario 1	1.97	2.34	2.51	2.90	3.88	4.19
	Scenario 2	1.87	2.18	2.28	2.71	3.64	4.00
	Scenario 3	1.63	1.98	2.05	2.47	3.28	3.70

[a] The 2055 sea level scenario shown here is the central estimate, the 50th percentile

Table 3: Flood area reduction (km^2) by scenario, storm return period and sea level year

	10-year		100-year		1000-year	
Scenario	**2016**	**2055**	**2016**	**2055**	**2016**	**2055**
Scenario 1	1.2	0.6	8.4	3.3	5.0	6.4
Scenario 2	8.7	2.1	10.1	6.7	10.1	12.4
Scenario 3	10.2	3.8	12.1	12.6	24.8	19.9

Table 4: Upland flood area reduction (%) by scenario, storm return period and sea level year

	10-year		100-year		1000-year	
Scenario	**2016**	**2055**	**2016**	**2055**	**2016**	**2055**
Scenario 1	42	11	51	13	9	9
Scenario 2	98	35	62	25	17	18
Scenario 3	97	63	73	49	42	28

[a] Tallied only for locations above 1.8 m navd88, a minimum elevation of residences around the bay

3.4 Influence of sea level rise on flood hazards and mitigation

Reductions in flood height will eventually be offset by any sea level rise, as shown by the flood maps in **Figures 11 and 12**, for mid-level estimates of sea level rise for 2055. Or, put more positively, the flood mitigation strategies are able to offset the effect on flooding of several decades of future sea level rise. The impacts of sea level rise (2016 to 2055; **Table 2**) are approximately linear or "static", meaning that a 45 cm sea level rise leads to approximately a 45 cm increase in flood height, and the same is observed with the adaptation scenarios. Therefore, considering the uncertainty range in sea level rise projections [10th to 90th percentile estimates; *Horton et al.*, 2015], the Scenario 3 reduction in the 100-year flood of 65 cm is equivalent to approximately 45-140 years of sea level rise, with the central estimate of 70 years.

Looking more broadly at the scenarios and storm events, mitigation scenario #2 reduces flood levels by 18 cm (average of the two locations in **Table 2**) for a 10-year flood, and 37 cm for the 100-year flood, which is equivalent to the effect of 24 and 45 years of sea level rise, respectively [by the 50th percentile within the NPCC projections; *Horton et al.*, 2015]. Mitigation scenario #3 reduces flood levels by 41 cm for a 10-year flood, and 65 cm for the 100-year flood, which is equivalent to 48 and 70 years of sea level rise (out to years 2065 and 2087, respectively).

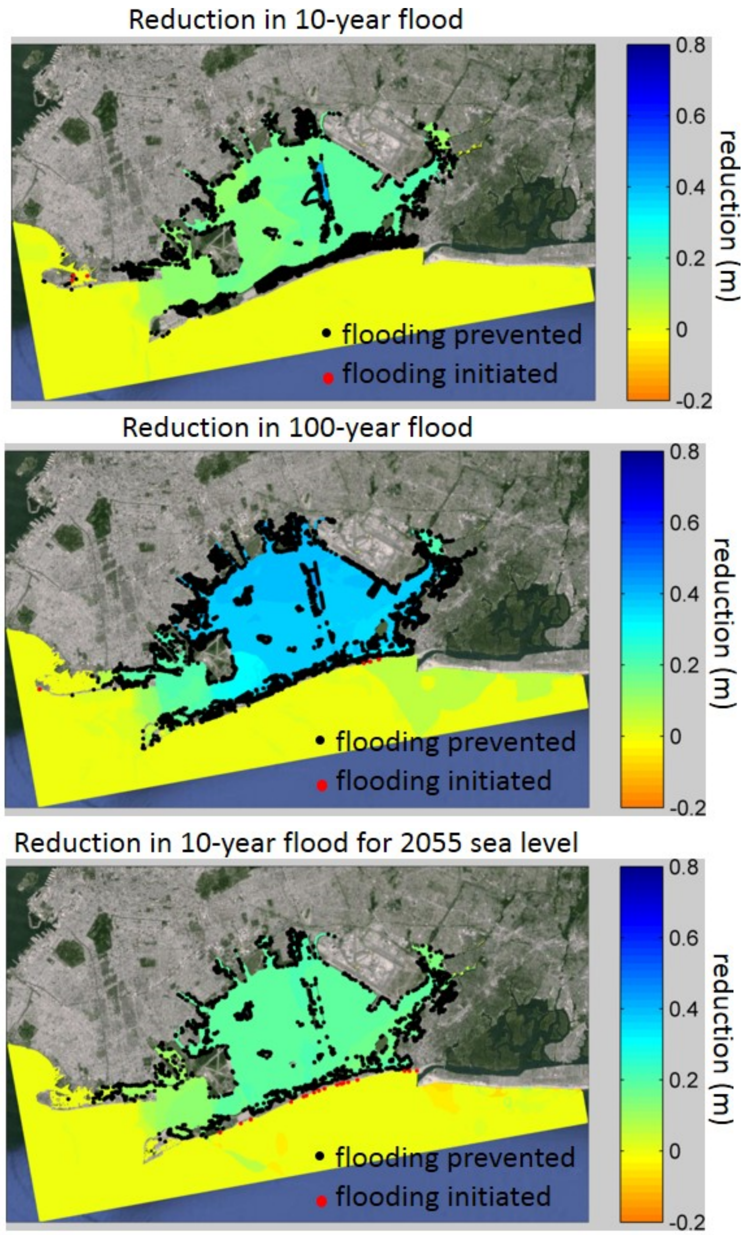

Figure 11: Flood elevation reductions for mitigation scenario #2 (narrowing and sand replenishment), showing the reductions for the 10-year and 100-year flood events, and the 10-year event with the median estimate of sea level rise for 2055. In areas with black dots, flooding is prevented due to the flood mitigation strategy, whereas in areas with red dots (very few) new flooding is initiated.

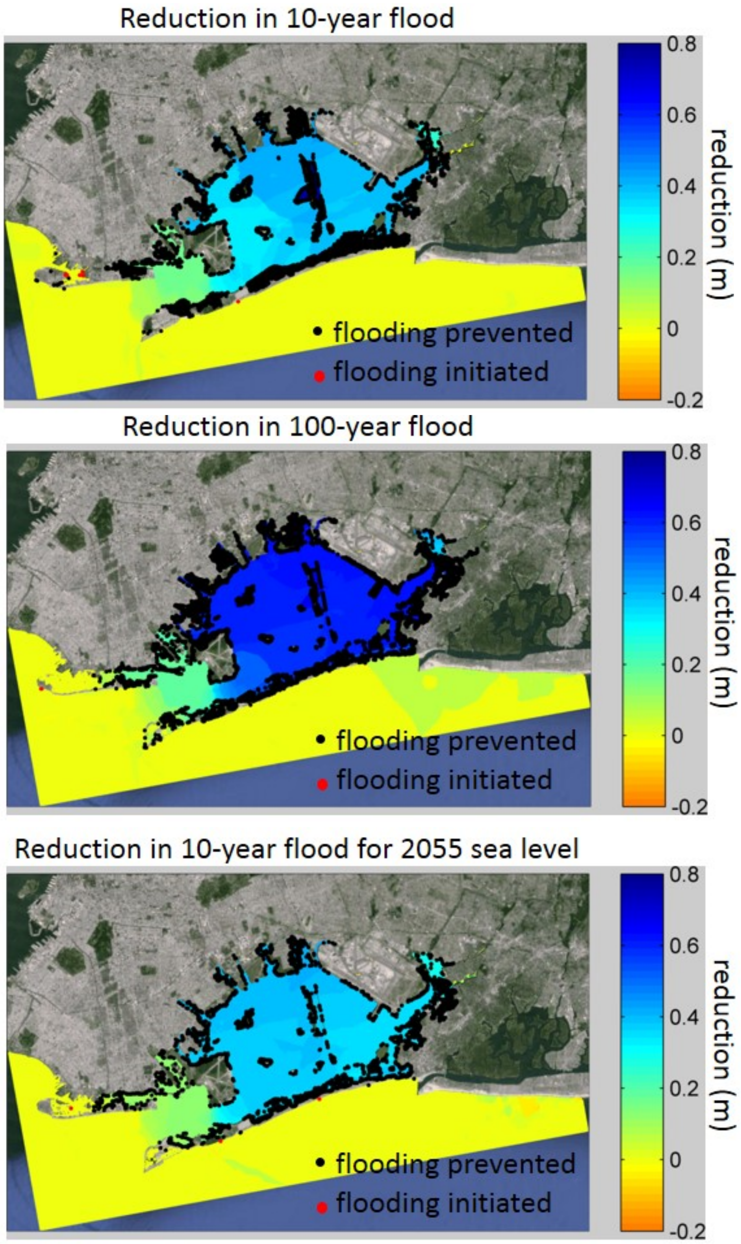

Figure 12: Flood elevation reductions for mitigation scenario #3, showing the reductions for the 10-year and 100-year flood events, and the 10-year event with the median estimate of sea level rise for 2055.

3.5 Mitigation cost estimation and benefit-cost analysis results

Mitigation measures were priced only by the cost of sand, assuming simple offshore dredge and pipe methods would be used to deliver sand from the continental shelf. An assumption here is that sand would be placed in the bay, and natural processes would be allowed to take over, so there would be no maintenance costs.

The average cost of sand for beach replenishment projects on the US East Coast surrounding New York Bight has been $17 per cubic meter. On the other hand, a recent study under the Housing and Urban Development competition Rebuild By Design also made an estimate based on Dutch dredge company costs of only $3.29-6.65 per cubic meter, though admitting it was speculative and optimistic .

For a final estimate, we interviewed Bill Hansen at the local office of the dredge company Great Lakes Dredge. He felt that the Blue Dunes study was likely underestimating costs by using European estimates that were unlikely to be achieved in the United States. He also explained the average cost of recent beach replenishment efforts was likely too high, and lower costs would be achieved through economies of scale (this would be a much larger project) and harnessing the latest technology. He provided a final estimate of $6-8 per cubic yard, which we apply to our study as a central estimate of $7 and a 80% confidence interval of $6-8.

Applying these estimates of costs, estimated damages avoided, and uncertainties, our results show that these nature-based adaptation options are cost effective and can reduce large amounts of flooding. All three scenarios have benefit-cost ratio (BCR) 80% confidence limits that are above 1, the level at which costs are balanced by benefits. This is found even for a high discount rate of 7%, and lower discount rates provide higher BCR values. Scenarios 1 and 2 have the highest BCRs, which for the intermediate discount rate of 5% are 2.9 (1.93-3.87) and 2.75 (1.82-3.68).

Table 5: The estimated benefit and benefit-cost ratio of each landscape. If a benefit-cost ratio is greater than one, the measure is cost effective.

Landscape	Discount rate	Benefit (millions $)	Benefit-Cost Ratio
Scenario 1	3%	1,069 (641 – 1,497)	3.87 (2.58–5.17)
	5%	800 (479 – 1,121)	2.9 (1.93–3.87)
	7%	627 (375 – 880)	2.27 (1.51–3.03)
Scenario 2	3%	2,137 (1,273 – 3,001)	3.68 (2.44–4.92)
	5%	1,594 (947 – 2,241)	2.75 (1.82–3.68)
	7%	1,246 (739 – 1,753)	2.15 (1.42–2.87)
Scenario 3	3%	3,152 (1,873 – 4,431)	2.74 (1.81–3.67)
	5%	2,344 (1,392 – 3,296)	2.04 (1.35–2.73)
	7%	1,827 (1,085 – 2,570)	1.59 (1.05–2.13)

3.6 Online flood adaptation mapper

AdaptMap is an online mapping tool which demonstrates how coastal flood zones will change with sea level rise and in each of the adaptation scenarios. AdaptMap displays historical landscapes for the years 1609 and 1877 with associated historical flood zones. Users of this free online resource are able to download the results of a benefit-cost analysis, the underlying GIS layers corresponding to each scenario, and this technical report. Moreover, users may view animations of how water elevation around Jamaica Bay changes over the course of a storm for each landscape, sea level, and storm tide scenario.

3.6.1 Framework Technologies

AdaptMap is a fully customized JavaScript application created using the ESRI's Web Appbuilder for ArcGIS (Developer Edition) and the ArcGIS API for Javascript. Underlying data services were created using ArcGIS for Server 10.3.1 and exposed as compliant and interoperable Open Geospatial Consortium (OGC) web map services (WMS) and ESRI mapping services.

The project outcomes, background information, and AdaptMap tutorial are presented in an ArcGIS Online (AGOL) Story Map. The story map also includes interactive features to allow for additional comparisons of landscapes and their mitigation potential.

3.6.2 Scenario Options

Users are able to select and view scenarios of interest through manipulating a series of slider controls; one with landscape options, another with sea level, and a third with storm tide. **Figures 13-15** below display the potential selections within each control.

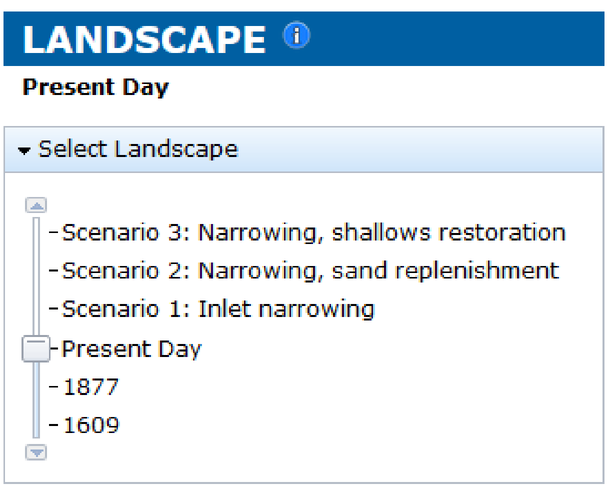

Figure 13: The landscape control includes options for present day plus three future adaptation scenarios: Scenario 1 Inlet Narrowing; Scenario 2 Narrowing, sand replenishment; and Scenario 3 Narrowing, shallows restoration, and two historic landscapes for the years 1609 and 1877.

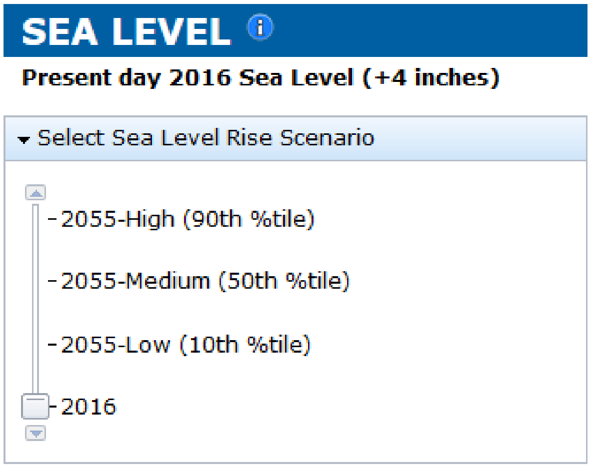

Figure 14: The sea level control is active when viewing the present day landscape or any of the three adaptation scenarios. The options consist of the 2016 sea level (+4 inches), the estimated 2055 sea level at the 10th percentile (+10 inches), the estimated 2055 sea level at the 50th percentile (+18 inches), and the estimated 2055 sea level at the 90th percentile (+32 inches). All sea levels rise projections are measured relative to the 1983-2001 base period, and are based on recent projections from the New York City Panel on Climate Change (Horton et al., 2015). When viewing a historic landscape, a default sea level is selected which is equal to the historic sea level for 1609, or 1877 respectively.

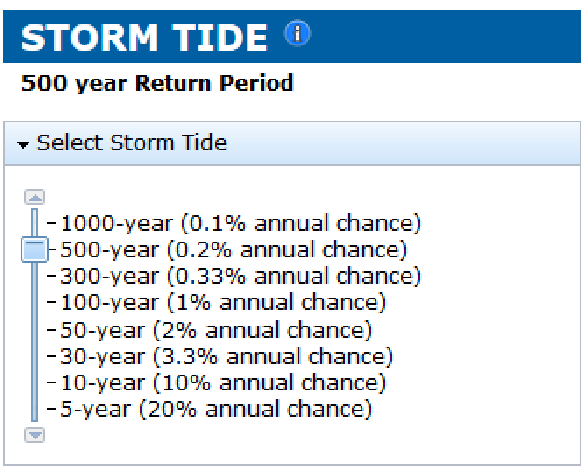

Figure 15: The storm tide control includes eight possible storm return periods: 5-year (20% annual chance), 10-year (10% annual chance), 30-year (3.3% annual chance), 50-year (2% annual chance), 100-year (1% annual chance), 300-year (0.33% annual chance), 500-year (0.2% annual chance), and 1000-year (0.1% annual chance).

3.6.3 Basemaps

Flood inundation extents selected on the basis of landscape, sea level, and storm tide scenarios are visualized as overlays on a variety of potential basemaps. The historical 1609 landscape has an accompanying basemap based on the landcover classification for 1609 desribed earlier in the report. The historical 1877 landscape has an accompanying basemap digitized from Bache [1882]. Present day and future landscapes provide a number of basemap possibilities. The ArcGIS Online mapping service provides ten global basemaps for use in web applications, and the Imagery with Labels basemap is the default for present day and future scenarios. Additionally, five custom basemaps leveraging the Critical Infrastructure database used in the BCA are available. They include the themes of Community Services, Emergency Services, School, Transportation, and Utilities and depict critical infrastructure locations.

3.6.4 Downloads

GIS Flood Data

This downloadable zip file includes a GeoTiff of the flooding in your selected scenario. The raster type file is provided in the UTM18N projection and is compatible with most open source and commercial desktop GIS packages. The vertical unit of the file is US Feet.

Detailed Report

The detailed report (the present document) presents an in depth look at the methods used to create the scenarios and assess the impacts contained within AdaptMap

Benefit-Cost Analysis

This downloadable Microsoft Excel file summarizes the results of the benefit-cost analysis of flooding under each Adaptation Scenario. You can also explore the detailed breakdowns of the implementation costs and estimated economic damages avoided for each Adaptation Scenario. This report also includes a full set of damage estimates for all scenarios.

4.0 Discussion and Conclusions

Our research in this project has led to several noteworthy accomplishments, including:

- Creation of Jamaica Bay water circulation models for present-day and historical landscapes (1609, 1877)
- Demonstration that floods in Jamaica Bay have been raised higher by widening and dredging Rockaway Inlet, presently 900-1100 km wide and 8-16 m deep off Floyd Bennett Field
- Development of new ideas for nature-based flood mitigation for an urban harbor
- We have created a new type of online tool– a flood adaptation mapper

The work has been improved along the way by government and community stakeholder input, and it continues to be. Our project's outputs serve our project title's objective of helping people visualize and quantify the benefits of natural features for flood adaptation for Jamaica Bay. The value of disseminating historical, present day, and future scenarios for public education and for decision-making cannot be understated, and this approach could reasonably be used in other geographic areas where similar mappers could be created. Below, some aspects of these accomplishments are discussed.

4.1 Storm tide amplification by the present-day landscape

Jamaica Bay has flooding problems for a few well-known reasons. Much of the landscape immediately surrounding the bay is landfilled wetlands, and is not highly elevated. These land areas may have soils that are compacting, lowering land elevations further. Also, sea level has locally risen by about one foot in the past century, due to land subsidence and global sea level rise.

However, our project shows that an additional reason for increased flooding is human alterations of the landscape. **Figure 9** clearly demonstrates the influence of these changes since 1877 on the 100-year flood, simulated on present-day mean sea level. Below in **Figure 16**, typical monthly high tide is mapped, based on modeling but also seen in sea level data at Inwood, Rockaway Inlet, and in prior published work [*Swanson and Wilson*, 2008]. Also in the right-hand panel, the 10-year flood is mapped, based on our flood hazard assessment, again showing higher water levels within the bay, versus outside it. These results demonstrate that areas around Jamaica Bay frequently flood because the landscape amplifies tides and storm surges in the bay.

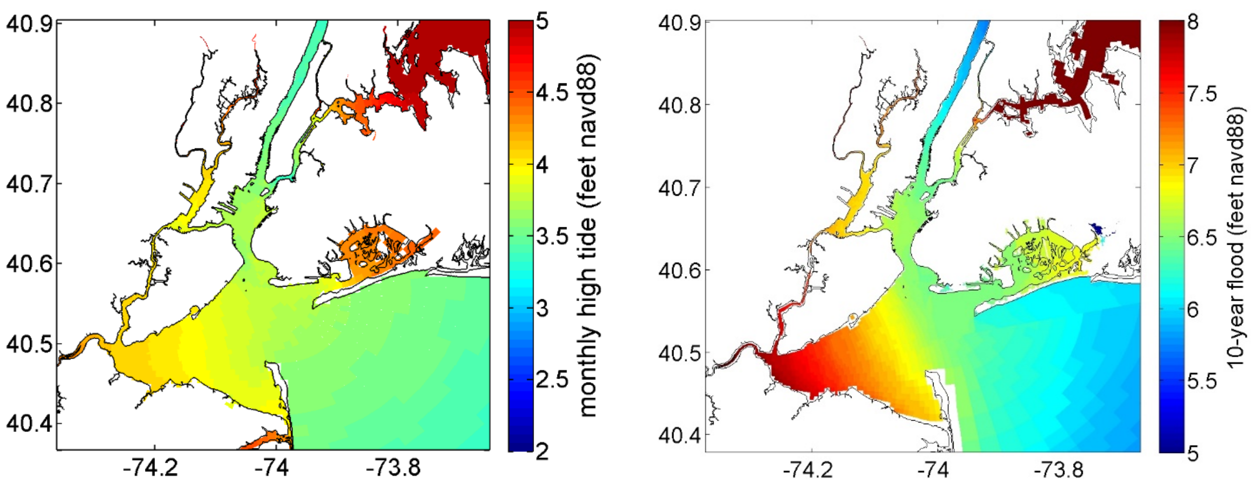

Figure 16: Model results for the present-day landscape and 2016 sea level, showing amplification of tides and storm tides in Jamaica Bay. (left) Typical monthly high tide, showing maximum water levels from a simulation of tides for August 2015. (right) The 10-year storm tide, based on the full probabilistic flood hazard assessment. Typical winds in a 10-year flood are from the east, which should blow water out of the bay, yet the water levels still rise with distance eastward in Jamaica Bay.

These results and those in **Figure 9** helped guide our adaptation designs for our project, as they show that a large part of the problem with Jamaica Bay flooding is amplification of tides and also in some cases, storm surges. Hurricane Sandy flood levels were actually lower in Jamaica Bay than they were to the west of the bay entrance or in New York Harbor. However, in general our work has shown clearly that the attenuation of storm tides is limited and in some cases there is amplification of storm tides. One interesting comparison is that relative sea level rise led to an increase of about 38 cm in flood levels from 1877 to 2016, whereas the modifications to the landscape have led to a 44 cm increase in the 100-year storm tide (**Figure 8**), thus the human-made changes to the landscape have caused more worsening of flooding than sea level rise.

Our results in **Figure 8** show that Jamaica Bay was once more of a shallow, back-bay system, protected by varying degrees historically by a barrier island, and has been converted into a deepwater port-type estuary system. Our flood mapping results are consistent with recent research showing how back-bay systems (e.g. Great South Bay, Barnegat Bay) attenuate rapid sea level events like tides and storm surges, whereas open port-type systems (e.g. New York Harbor) do not [*Aretxabaleta et al.*, 2014]. The impact of these changes has been an elimination of much of this natural protective benefit. This greater understanding of how the system has changed and why it is vulnerable to flooding opens up new possibilities for future flood mitigation.

Quantitative estimates of the inlet cross-sectional area (CSA) provide a measure of how much the inlet has changed. The minimum CSA of our present-day inlet in this project's model grid is at Floyd Bennett Field and is 8100 m^2 (at the 2016 mean sea level). The minimum CSA in the inlet for our 1877 our grid (at an 1877 sea level) is 4700 m^2. And lastly, the minimum CSA in 1844 was approximately 3800 m^2 (based on the Hassler map, correcting MLLW to MSL using an offset of 0.69 m). An updated model grid we have produced under National Parks Service funding subsequent to the modeling done for this project utilizes the most up-to-date bathymetric data for the inlet, collected by Stony Brook's Roger Flood and others around ~2010 and only recently made public. This new grid shows the inlet in "present-day" is actually deeper than the outdated bathymetric data showed, with a cross-sectional area of 8920 m^2. In conclusion, the inlet has more than doubled in size since the mid-1800s (increased by a factor of 2.35 since 1844, or 1.90 since 1877), greatly increasing the conveyance of storm surges and tides into the bay.

4.2 Novel, cost-effective, nature-based flood mitigation approaches for urban harbors

A major achievement in this project has been the development of a class of entirely new ideas for flood mitigation for deep-water harbors, which might be contrasted against "grey" and "green" flood adaptation as "beige" flood adaptation, relating to the color of sand.

The narrowing and shallowing approaches tested here demonstrate sizeable reductions in flood risk, as exemplified with Scenario 2 by the elimination of neighborhood flooding for the 10-year storm event and the moderate reduction in levels (30 cm) for the 100-year flood event. This scenario is realistic on a multi-year timescale, and the benefit-cost ratios of ~3 for narrowing (Scenario 1) and narrowing and shallowing (Scenario 2) demonstrate that these approaches are cost effective (**Table 5**).

These techniques are somewhat simplistic, and due to the small size of our project they have not been subjected to a wider analysis nor significant efforts for optimization. For example, optimization could address any or all of the multiple goals of flood risk reduction, water quality improvement, recreational use, shipping, habitat (e.g. wetlands), and fishing. The cumulative nature of the three scenarios does lay out a possible pathway for applying these ideas gradually and building the flood resilience up over many decades.

Sea level rise is an important additional consideration for flood mitigation in the coming decades, particularly as the rate of sea level rise accelerates above the current local rate of ~4 cm per decade. A detailed summary of how the flood reductions perform and compare with sea level rise is given in **Section 3.4**. To summarize, Scenario 3 causes reductions in the 100-year flood of 50-60 cm, which is equivalent to eliminating the future effects of 40-130 years of sea level rise.

There are also potential ecological benefits for shallowing Jamaica Bay. Filling in the borrow pits, large deepwater areas deep inside the bay with low oxygen levels, is a well-established strategy for improving oxygen levels in the bay that has not yet won approval, but could be beneficial. Also, the Bay is likely at a deficit for sand supply, with sediment being imported, but at too low a rate to allow islands and wetlands to rise with present-day sea level rise. Evidence for this begins with the fact that the marsh island area has been collapsing in recent decades. Further evidence was provided at the 2016 State of the Bay Symposium, where an observational study and a modeling study were both referenced to support the estimate that the sediment inputs are about 5 times too low [Chant, 2016]. Adding sand directly into the bay could help improve the sediment budget for these wetlands, so that during storms there may be sediment resuspension and settling on top of the wetlands substrate. Or, the new sediment could simply be pumped up and blown over the marsh islands to directly help maintain their elevation.

4.3 Flood adaptation mappers

The AdaptMap flood adaptation mapper is one of very few online flood mapping tools that maps the results of dynamic modeling. Most other flood scenario mappers (e.g. Climate Central's popular and useful Surging Seas tool) provide information based on static flood mapping, where water is assumed to behave simply and only rise and spread horizontally and uniformly over land. Dynamic flood maps require hydrodynamic modeling that accounts for all the forces impacting the water, and thus a great deal of computational time – this project utilized a supercomputer system at City University of New York and required about 300,000 cpu-hours of computational power. The results are analyzed, flood probabilities computed, and resulting simplified estimates of flood heights placed into the tool for rapid retrieval. GIS Flood data and benefit-cost analysis results are available for user download.

Dynamic flood mappers have many enhanced capabilities, relative to static flood mappers. These include the capacity to show how obstruction, constriction, or vegetation in an area can reduce flooding, the ability to convey the temporal nature of flooding through the use of flood event animations that convey the speed at which the flood recedes following an event. This is especially important to understand in concave or leveed-in neighborhoods, where flood waters often remain for long periods after the storm has passed (e.g. New Orleans after Katrina). Dynamic flood mappers can display modeling results that incorporate a wide range of complex factors for flooding, including local winds, sea level rise, rainfall, and the future response of coastal wetlands to sea level rise which may disappear if their substrate cannot rise with sea level rise. Another example of a dynamic flood mapper created by this project team is the Hudson River Flooding Decision Support System [http://www.ciesin.columbia.edu/hudson-river-flood-map/], which merges effects of rainfall, snowmelt, sea level rise, tides and storm surge into one mapping tool.

A shortcoming of a dynamic flood mapper is that its computationally-expensive modeling requires a relatively low-resolution landscape relative to what is often available (e.g. 1 m LIDAR data). In this study's case the model resolution is 30 m. This can lead to inaccurate flow pathways in cases where the landscape has smaller features such as elevated seawalls, though these are rare around Jamaica Bay. This complicates the question of whether dynamic or static mapping of sea level rise is more accurate. However, the many advantages listed above are reasons why dynamic flood mappers and adaptation mappers are likely to become more common.

4.4 Contrasting a storm surge barrier and nature-based flood mitigation strategies

The narrowing and shallowing approaches to flood mitigation presented in this study could be further developed and optimized to provide actionable plans for reducing flood risk around Jamaica Bay. These strategies could considered as supplements or alternatives to the storm surge barrier plan that the Corps of Engineers is releasing as their "preferred alternative". That plan is for a barrier in the region of Rockaway Inlet off Floyd Bennett Field, which would generally be left open except during storm surge events.

As a compliment to a surge barrier, the narrowing strategy could use the narrowing strategy off Coney Island/ Brighton Beach along with the choking of water flow from the barrier structure's supports off Floyd Bennett Field, instead of narrowing with sand or other nature-based features at that location. The barrier's structures will have similar effects as our narrowing at that location, and the expense of the barrier actually goes down as the level of obstruction goes up (gates cost more money and allow more flow). Inlet narrowing, along with some amount of shallowing perhaps similar to our Scenario 2, could prevent flooding from 10-year and smaller floods for coming decades, letting the Corps leave the gates open during smaller flood events. In this way, the natural system could be partially restored (e.g. a smaller inlet, increased sand in the bay) and allowed to reduce flooding with natural processes during smaller flood events. The gate could be closed during larger events, protecting the population from severe events and damages.

The progression from Scenarios 1 to 2 to 3 could also be viewed as an alternative to a surge barrier plan. These strategies are demonstrated in this project to be moderately effective flood risk reducers, and are able to offset the effects on flooding of several decades of sea level rise.

There is no flood reflection with shallowing and narrowing, no net increase in flood area outside of the bay. In contrast, we have performed model experiments using ADCIRC with Hurricane Sandy that show that the surge barrier system would increase flood elevations outside the bay, including ~5 cm increases off Manhattan on the Hudson River. The increases in flood elevations outside the barrier system are not surprising, given the huge quantity of water that is prevented from entering the bay. Our shallowing and narrowing strategies do not block water, they slow it, and thus they do not cause significant flood reflection or additional flooding.

The Corps of Engineers Rockaway Reformulation study recently evaluated a complete set of flood mitigation options for Jamaica Bay [*USACE*, 2014]. Early in the process, the concept of shallowing the bay was struck from the list mainly based on evidence that it would be too expensive, yet the report contains a factor of ten error in the cost computation. The consulting firm who led the study has conceded that this was an error. The Corps was under pressure to move forward quickly with present understanding and without time for new science, presumably due to the goal of capturing post-Sandy funding. As a result of these developments, new ideas like shallowing or narrowing were not considered in the subsequent analysis that concluded that a storm surge barrier was the best solution for flood mitigation at Jamaica Bay.

4.5 Project shortcomings and next steps

Some shortcomings of our study are noted here, but also additional research is outlined that will address these limitations. The study is focused only on still-water flood elevation, so ignores waves and the reductions in waves from nature-based features (e.g. wetlands). However, we are looking at wave crest height and wave attenuation by vegetation in a separate project (see below). The study looks at flood elevations and area, but neglects to consider broader impacts of mitigation strategies like shallowing, which could choke flow in and out of the bay and harm water quality. However, we are also studying water quality, dynamic vegetation evolution, in a subsequent study (again, see below). This study uses two-dimensional (2D) modeling of water flows, whereas three-dimensional (3D) modeling is more accurate. In particular, the 2D modeling uses simplistic treatment of vegetation as roughness elements on a flat plane. However, we have subsequently developed 3D vegetation-flow-wave modeling capabilities in a subsequent project (below). Lastly, this project's benefit-cost analysis lacks ecosystem services, but we have new funding to address this.

This project was selected for funding in 2013 and performed from January 2014 to summer 2016, but three additional projects have been funded since its initiation. These studies are enabling us to continue with related research, including deeper analyses of the flood mitigation concepts presented here. The general concepts of flood mitigation developed under this project have also been accepted as worth further evaluation by stakeholders, within stakeholder input meetings under these other projects. Research areas that are receiving further attention under these new projects include: (1) the water quality impacts of flood mitigation efforts, (2) impacts on waves of a range of nature-based flood mitigation strategies, and (3) the incorporation of a wider range of ecosystem benefits into decision-making.

One project, "Coastal Adaptation Impacts on Jamaica Bay Water Quality, Waves and Flooding" was funded by the National Parks Service from 2015-2016 (P. Orton, Stevens Institute, lead-PI). The primary goals in the project are to: Improve the existing water quality modeling in Jamaica Bay (J-Bay) with enhanced model representations of wetlands, macro-algae, and wetland and benthic chemical/nutrient fluxes; Improve hydrodynamic model representations of J-Bay wetlands and air-sea interaction; Utilize higher-resolution modeling in the bay and improve modeling of exchanges with the coastal ocean by coupling the J-Bay models with inputs from regional scale models; Calibrate the improved models using data collected by the consortium and USGS in J-Bay; Run experiments to study climate change, sea level rise and coastal adaptation impacts on flooding, waves, water quality and residence time.

Also, Wildlife Conservation Society and others are funded by Rockefeller Foundation for a study called "Towards a Jamaica Bay Master Plan". Under this project, we are evaluating how habitat areas such as wetlands respond to the flood mitigation strategies and climate change impacts, including how sea level rise dynamically alter the bay's tides and how the vegetated areas respond. We are also evaluating how flood mitigation and climate change influence residence times and water quality.

And lastly, "Incorporating Interactive Visions and Bioeconomic Values of Ecosystem Services into Climate Adaptation" (C. Bond, RAND Inc, lead-PI) is funded by NOAA's Coastal Ocean Climate Applications program for two years, beginning in summer 2016. Under this project, we will develop an improved Ecosystem Services valuation framework for Natural and Nature-Based Feature (NNBF) coastal flood adaptations, and we will incorporate the results into an interactive Ecosystem Services scenario modelling tool, Visionmaker.nyc. This work will lead to improved accounting for benefits of ecosystems that go beyond the damages avoided which were the sole benefit quantified in our BCA in the present study.

Acknowledgements

The authors would like thank all the project advisory committee members, who helped guide the project. Some particularly helpful or inquisitive members were: Ellen Hartig, Dan Mundy Jr., Dan Mundy Sr., Klaus Jacob, Peter Weppler, Barry Pendergrass, Radley Horton, Doug Marcy, Nicholas Schmidt, Jessica Fain, Marit Larsen, Pippa Brashear, Adam Parris, Jeanne DuPont, Carolyn LaBarbiera, Ben Strauss, and Ben Horton. Funding for this project was provided by the NOAA-CPO-CSI-COCA project "Quantifying the Value and Communicating the Protective

Services of Living Shorelines Using Flood Risk Assessment", award NA13OAR4310144. Additional funding for tropical cyclone flood modeling came from a NASA research project, "Inundation Hazard Assessment for New York City from Hurricane Storm Surge, Rainfall, and Climate Change" (agreement NNX15AD61G). Computer modeling was made possible, in part, by a grant of computer time from the City University of New York High Performance Computing Center under NSF Grants CNS-0855217, CNS-0958379 and ACI-1126113. Lastly, we would like to acknowledge the early and crucial role of Mark G. Becker (1961-2014), an original Principal Investigator for this project.

References

Aerts, J., W. W. Botzen, K. Emanuel, N. Lin, H. de Moel, and E. O. Michel-Kerjan (2014), Evaluating Flood Resilience Strategies for Coastal Megacities, *Science*, *344*(6183), 473-475.

Allen, D. Y. (1998), The Enigmatic Topographic Maps of the U.S. Coast Survey, 1834-1861, *Meridian*, *13*, 42–60.

Anonymous (1783), British Headquarters Map, The National Archives, Kew, United Kingdom.

Aretxabaleta, A. L., B. Butman, and N. K. Ganju (2014), Water level response in back-barrier bays unchanged following Hurricane Sandy, *Geophys. Res. Lett.*, *41*(9), 3163-3171.

Avila, L. A., and J. Cangialosi (2011), Tropical Cyclone Report: Hurricane Irene (AL092011)*Rep.*, 45 pp, National Hurricane Center.

Bache, A. D. (1861), New York Bay and Harbor, New York, Survey of the Coast of the United States, Coast Chart No. 21, Washington D.C.

Bache, A. D. (1882), New York Bay and Harbor, New York, Coast Chart No. 20, Survey of the Coast of the United States, Washington D.C. .

Bellot, A. H. (1917), *History of the Rockaways from the year 1685 to 1917: being a complete record*, Bellot's Histories, Far Rockaway, New York.

Bien, J. R., and C. C. Vermeule (1891a), Jamaica Bay, Atlas of the Metropolitan District and adjacent country, Julius Bien & Co, New York.

Bien, J. R., and C. C. Vermeule (1891b), The Narrows to Jamaica Bay-Coney Island, north to Brooklyn, Atlas of the Metropolitan Area and Adjacent Country, Julius Bien & Co, New York.

Black, F. R. (1981), *Jamaica Bay: A History (Cultural Resource Management Study No. 3)*, Washington, D.C.

Bromberg, K. D., and M. D. Bertness (2005), Reconstructing New England salt marsh losses using historical maps, *Estuaries*, *28*(6), 823-832.

Dahl, T. E. (2006), *Status and trends of wetlands in the conterminous United States 1998 to 2004*, 112 pp., Washington, D.C.

Dorr, F. W. (1859), Map of Part of Brooklyn Including Williamsburg & Green Point, To Join the City as Laid Out by the City Surveyors (U.S. Coastal Survey T-Sheet 789), U.S. Coast Survey, Washington, D.C.

Dorr, F. W. (1860), Part of Far Rockaway, Long Island (U.S. Coast Survey T-Sheet 798), U.S. Coast Survey, Washington, D.C.

Eddy, J. H. (1811), Map of the Country Thirty Miles Round the City of New York., J. Eddy, New York.

Edinger, G. J., D.J. Evans, S. Gebauer, T.G. Howard, D.M. Hunt, and A.M. Olivero (2014), *Ecological Communities of New York State: Second Edition, A Revised and Expanded Edition of Carol Reschke's Ecological Communities of New York State*, NYS Department of Environmental Conservation, Albany, NY.

ESRI (2016), How Topo to Raster works—Help | ArcGIS for Desktop, http://pro.arcgis.com/en/pro-app/tool-reference/3d-analyst/how-topo-to-raster-works.htm, accessed June 29, 2016.

FEMA (2013), Federal Emergency Management Agency Modeling Task Force (MOTF)-Hurricane Sandy Impact Analysis, https://data.femadata.com/MOTF, accessed March 13, 2016.

FEMA (2014), Final Draft Report: Region II Coastal Terrain Processing Methodology Documentation Report*Rep.*, 48 pp, prepared by Risk Assessment, Mapping, and Planning Partners (RAMPP), Washington, DC.

Georgas, N., P. Orton, A. Blumberg, L. Cohen, D. Zarrilli, and L. Yin (2014), The impact of tidal phase on Hurricane Sandy's flooding around New York City and Long Island Sound, *Journal of Extreme Events*, doi:10.1142/S2345737614500067.

Giampieri, M., and E. Sanderson (in preparation), Quantification of pre-urbanization coastal dynamics of the Rockaway Peninsula and Coney Island barrier system in New York City.

Gilbert, S. A. (1855a), Coney Island and Dead Horse Inlet (U.S. Coast Survey T-Sheet 586), U.S. Coast Survey, Washington, D.C.

Gilbert, S. A. (1855b), Western End of Long Island from Gowanus Bay to Bath (U.S. Coast Survey T-Sheet 487), U.S. Coast Survey, Washington, D.C.

Gilbert, S. A. (1856a), Gowanus Bay and Vicinity, Long Island (U.S. Coast Survey T-Sheet 597), U.S. Coast Survey, Washington, D.C.

Gilbert, S. A. (1856b), Gowanus Bay and Vicinity, Long Island (U.S. Coast Survey T-Sheet 598), Washington, D.C.

Gilbert, S. A., and J. A. Sullivan (1857), Gowanus Bay and Vicinity, Long Island (U.S. Coast Survey T-Sheet 599), U.S. Coast Survey, Washington, D.C.

Gormley, M. (2012), Cuomo: Sandy Cost NY, NYC $32B in Damage and Loss, The Big Story, Associated Press.

Grossinger, R. M., R. A. Askevold, and J. N. Collins (2005), T-Sheet User Guide: Application of the Historical U.S. Coast Survey Maps to Environmental Management in the San Francisco Bay Area.

Guthorn, P. J. (1984), United States Coastal Charts, 1783-1861, Schiffer Publishing, Exton, PA.

Hassler, F. R. (1844), Map of New-York Bay and Harbor and the Environs, United States Coast Survey, Washington, D.C.

Homer, C. G., J. A. Dewitz, L. Yang, S. Jin, P. Danielson, G. Xian, J. Coulston, N. D. Herold, J. Wickham, and K. Megown (2015), Completion of the 2011 National Land Cover Database for the conterminous United States-Representing a decade of land cover change information, *Photogramm. Eng. Remote Sens*, *81*(5), 345-354.

Horton, R., V. Gornitz, M. Bowman, and R. Blake (2010), Chapter 3: Climate observations and projections, In: (Rosenzweig, C. and Solecki, W., Eds.) Climate Change Adaptation in New York City: Building a Risk Management Response, *Ann. N. Y. Acad. Sci.*, *1196*(1), 41-62, doi:10.1111/j.1749-6632.2009.05314.x.

Horton, R., C. Little, V. Gornitz, D. Bader, and M. Oppenheimer (2015), New York City Panel on Climate Change 2015 report Chapter 2: Sea level rise and coastal storms, *Ann. N. Y. Acad. Sci.*, *1336*(1), 36-44.

Jeffries, J. (2011), Property Claim Services Increases Irene Damage Estimates to $4.3 Billion, in *Insurance News Net*, November 29, 2011.

Jenkins, T. A. (1837a), Map of the Interior of Long Island from Brooklyn to Jaimaica, New York (U.S. Coast Survey T-Sheet 36), U.S. Coast Survey, Washington, D.C.

Jenkins, T. A. (1837b), Map of the Interior of Long Island from Brooklyn to Jaimaica, New York (U.S. Coast Survey T-Sheet 37), Washington, D.C.

Kemp, A. C., and B. P. Horton (2013), Contribution of relative sea-level rise to historical hurricane flooding in New York City, *Journal of Quaternary Science*, *28*(6), 537-541.

Koks, E. E., M. Bočkarjova, H. de Moel, and J. C. J. H. Aerts (2015), Integrated Direct and Indirect Flood Risk Modeling: Development and Sensitivity Analysis, *Risk Analysis*, *35*, 882–900, doi:10.1111/risa.12300.

Maynard, W. (1877), Western Part of Jamaica Bay Including Canarsie Landing (U.S. Coast Survey H01358), U.S. Coast Survey, Washington, D.C.
Moore, W. I. (1878), Jamaica Bay Eastern Part (U.S. Coast Survey H01392), Washington D.C.
Munsell, W. W. (1882), *History of Queens County, with illustrations, Portraits &Sketches of Prominent Families and Individuals*, W.W. Munsell & Co., New York.
NOAA-NCDC (2011), *Storm Data and Unusual Weather Phenomena, 53, 8,*, National Oceanic and Atmospheric Administration \ National Climatic Data Center, Asheville, NC.
NOAA (2015), Tides and Currents, National Oceanographic and Atmospheric Administration, https://tidesandcurrents.noaa.gov/, accessed 2016 October 1.
NRC (2005), *Valuing ecosystem services: Toward better environmental decision-making.*, National Academy Press, National Research Council, Washington, D.C.
NYC-DEP (2007), Jamaica Bay Watershed Protection Plan, Volume 1, p. 128, New York City Department of Environmental Protection (DEP), New York, NY, USA.
Olsen, A. S., Q. Zhou, J. J. Linde, and K. Arnbjerg-Nielsen (2015), Comparing Methods of Calculating Expected Annual Damage in Urban Pluvial Flood Risk Assessments, *Water*, *7*, 255-270.
Orton, P., N. Georgas, A. Blumberg, and J. Pullen (2012), Detailed modeling of recent severe storm tides in estuaries of the New York City region, *J. Geophys. Res.*, *117*, C09030, doi:10.1029/2012JC008220.
Orton, P. M., T. M. Hall, S. Talke, A. F. Blumberg, N. Georgas, and S. Vinogradov (submitted), A Validated Tropical-Extratropical Flood Hazard Assessment for New York Harbor, *J. Geophys. Res.*
Orton, P. M., S. A. Talke, D. A. Jay, L. Yin, A. F. Blumberg, N. Georgas, H. Zhao, H. J. Roberts, and K. MacManus (2015), Channel Shallowing as Mitigation of Coastal Flooding, *Journal of Marine Science and Engineering*, *3*(3), 654-673, doi:10.3390/jmse3030654.
Orton, P. M., and Z. Wu (2015), Dynamic Modeling of Nature-Based Flood Adaptation Scenarios for Jamaica Bay, p. 39, Stevens Institute of Technology.
Ostrander, S. M. (1894), *A History of the City of Brooklyn and Kings County*, Annie A. Ostrander, New York.
Powell, J. W. (1891), USGS Brooklyn NY Quadrangle, U.S. Geological Survey, Washington, D.C.
Purchas, S. (1625), *Hakluytus Posthumus or Purchas His Pilgrimes: Contayning a History of the World in Sea Voyages and Lande Travells by Englishmen and others, Volumes XIII and XIV.*, J. Maclehose and Sons.
Resio, D. T., and J. J. Westerink (2008), Modeling the physics of storm surges, *Phys. Today*, *61*, 33-38.
Rockwell, C., and H. L. Whiting (1858), Map of the North Shore of Long Island from Little Neck Bay to Flushing Bay (U.S. Coast Survey T-Sheet 605), U.S. Coast Survey, Washington, D.C.
Sanderson, E. W. (2009), *Mannahatta: A Natural History of New York City*, Abrams, New York, NY.
Sanderson, E. W. (2016), Cartographic Evidence for Historical Geomorphological Change and Wetland Formation in Jamaica Bay, New York, *Northeastern Naturalist*, *23*(2), 277-304.
Sanderson, E. W., and M. Brown (2007), Mannahatta: An Ecological First Look at the Manhattan Landscape Prior to Henry Hudson, *Northeastern Naturalist 14*, 545–570.
Sandy Funding Tracker (2016a), Build it Back Single-Family and Multi-Family, http://www1.nyc.gov/sandytracker, accessed March 20, 2016.
Sandy Funding Tracker (2016b), Estimated Facility Damages, http://www1.nyc.gov/sandytracker, accessed April 1, 2016.

Scileppi, E., and J. P. Donnelly (2007), Sedimentary evidence of hurricane strikes in western Long Island, New York, *Geochem. Geophys., Geosyst.*, *8*(6), doi:10.1029/2006GC001463.
Shalowitz, A. L. (1964), Shore and Sea Boundaries with Special Reference to the Interpretation and Use of Coast and Geodetic Survey Data (Volume 2), United States Government Printing Office, Washington D.C.
Stiles, H. R. (1870), A history of the city of Brooklyn: including the old town and village of Brooklyn, the town of Bushwick, and the village and city of Williamsburgh, Published by subscription, New York.
Swanson, L., M. Dorsch, M. Giampieri, P. Orton, A. Parris, and E. W. Sanderson (2016), Chapter 4: Dynamics of the biophysical systems of Jamaica Bay, in *Prospects for Resilience: Insights from New York City's Jamaica Bay*, edited by E. W. Sanderson, W. D. Solecki., J. R. Waldman and A. S. Parris, Island Press, Washington, D.C.
Swanson, R., A. West-Valle, and C. Decker (1992), Recreation vs. waste disposal: The use and management of Jamaica Bay, *Long Isl. Hist. J.*, *5*(1), 21-41.
Swanson, R. L., and R. E. Wilson (2008), Increased tidal ranges coinciding with Jamaica Bay development contribute to marsh flooding, *J. Coast. Res.*, 1565-1569.
Taney, N. E. (1961), Geomorphology of the South Shore of Long Island, New York (No. Technical Memorandum 128), U.S. Army Corps of Engineers, Beach Erosion Board.
Tittman, O. H. (1907), Coast Chart No. 120. New York Bay and Harbor, New York, U.S. Coast and Geodetic Survey, Washington D.C.
US-HUD (2013), Sandy Damage Estimates Based on FEMA IA Registrant Inspection Data, US Department of Housing and Urban Development, https://www.data.gov, accessed April 15, 2016.
US-SBA (2011), SBA Disaster Loan Data FY11, U.S. Small Business Administration, https://www.sba.gov/, Accessed March 15, 2016.
US-SBA (2012), SBA Disaster Loan Data Superstorm Sandy, U.S. Small Business Administration, https://www.sba.gov/, accessed 15 March, 2016.
USACE (1963), Interim Survey Report, Morgan City, Louisiana and Vicinity, in *serial no. 63*, U.S. Army Corps of Engineers District, New Orleans, LA.
USACE (2014), East Rockaway Inlet to Rockaway Inlet and Jamaica Bay Reformulation Study, Memorandum for Record #1: Determination of Suitable Measures, PIKA Contract W91278-11-D-0101, TO CE01, United States Army Corps of Engineers.
Whiting, H. L. (1850), Re-Survey of City Id. Hart Id. and Hewlletts Point (U.S. Coast Survey T-Sheet 33 bis), U.S. Coast Survey, Washington, D.C.
Whiting, H. L. (1862), Interior of Long Island, New York, between Brooklyn, Flushing, and Jamaica (U.S. Coast Survey T-Sheet 924), U.S. Coast Survey, Washington, D.C.
Wilson, H. M. (1897), Hempstead NY Quadrangle, U.S. Geological Survey, Washington, D.C.
Zu Ermgassen, P. S. E., M. D. Spalding, B. Blake, L. D. Coen, B. Dumbauld, S. Geiger, J. H. Grabowski, R. Grizzle, M. Luckenbach, and K. McGraw (2012), Historical ecology with real numbers: past and present extent and biomass of an imperilled estuarine habitat, *Proceedings of the Royal Society B: Biological Sciences*, *279*(1742), 3393-3400.